As mentioned before, surface tension plays a large role in the mixing process, especially when dealing with dispersive mixing, when the capillary number approaches its critical value. Because of the stretching of the interfacial area, due to distributive mixing, the local radii of the suspended components decrease, causing surface tension to play a role in the process. It should also be noted that once the capillary number assumes a value below the critical *Ca*, only slight deformations occur and internal circulation maintains an equilibrium elliptical droplet shape in the flow field as schematically represented in Fig. 6.34. At that point, the mixing process reduces to the distribution of the dispersed droplets. Analytical and numerical investigations of stable droplet shapes, for $Ca < Ca_{crit}$ in simple shear flow have been made by several investigators [15–17]. Figure 6.32 also shows that at viscosity ratios above 4 simple shear flows are not able to break-up fluid droplets.

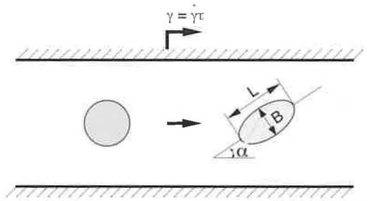

Figure 6.34 Schematic of droplet deformation in simple shear flow.

6.2.3 Mixing Devices

The final properties of a polymer component are heavily influenced by the blending or mixing process that takes place during processing or as a separate step in the manufacturing process. As mentioned earlier, when measuring the quality of mixing it is also necessary to evaluate the efficiency of mixing. For example, the amount of power required to achieve the highest mixing quality for a blend may be unrealistic or unachievable. This section presents some of the most commonly used mixing devices encountered in polymer processing.

In general, mixers can be classified in two categories: internal batch mixers and continuous mixers. Internal batch mixers, such as the Banbury type mixer, are the oldest type of mixing devices in polymer processing and are still widely used in the rubber compounding industry. Industry often also uses continous mixers because they combine mixing in addition to their normal processing tasks. Typical examples are single and twin screw extruders that often have mixing heads or kneading blocks incorporated into their system.

6.2.3.1 Static Mixers

Static mixers or motionless mixers are pressure-driven continuous mixing devices through which the melt is pumped, rotated, and divided, leading to effective mixing without the need for movable parts and mixing heads. One of the most commonly used static mixers is the twisted tape static mixer schematically shown in Fig. 6.35. Figure 6.36 [19] shows computed streamlines relative to the twist in the wall. As the fluid is rotated by the dividing wall, the interfaces between the fluids increase. The interfaces are then re-oriented by 90° once the material enters a new section. Figure 6.36 shows a typical trajectory of a particle as it travels on a streamline in section N of the static mixer and ends on a different streamline after entering the next section, N+1. The stretching-re-orientation sequence is repeated until the number of striations is so high that a seemingly homogeneous mixture is achieved. Figure 6.37 shows a sequence of cuts down a Kenics static mixer[5]. From the figure it can be seen that the number of striations increases from section to section by 2, 4, 8, 16, 32, etc., which can be computed using

$$N = 2^n \tag{6.17}$$

where N is the number of striations and n is the number of sections in the mixer.

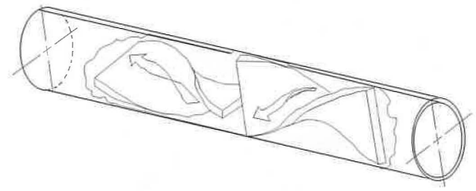

Figure 6.35 Schematic diagram of a Kenics static mixer.

[5] Courtesy Chemineer, Inc., North Andover, Massachusetts.

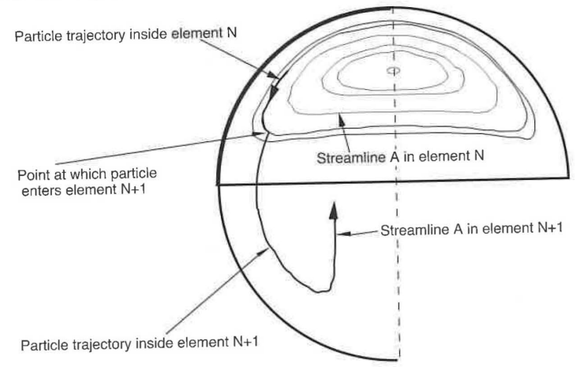

Figure 6.36 Simulated streamlines inside a Kenics static mixer section.

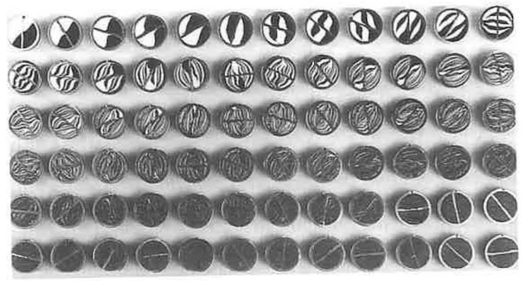

Figure 6.37 Experimental progression of the layering of colored resins in a Kenics static mixer.

6.2.3.2 Banbury Mixer

The Banbury type mixer, schematically shown in Fig. 6.38, is perhaps the most commonly used internal batch mixer. Internal batch mixers are high intensity mixers that generate complex shearing and elongational flows which work especially well in the dispersion of solid particle agglomerates within polymer matrices. One of the most common applications for high intensity internal

batch mixing is the break-up of carbon black agglomerates into rubber compounds. The dispersion of agglomerates is strongly dependent on mixing time, rotor speed, temperature, and rotor blade geometry [18]. Figure 6.39 [15, 21] shows the fraction of undispersed carbon black as a function of time in a Banbury mixer at 77 rpm and 100 °C. The broken line in the figure represents the fraction of particles smaller than 500 nm.

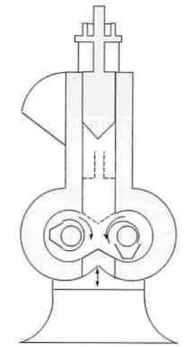

Figure 6.38 Schematic diagram of a Banbury type mixer.

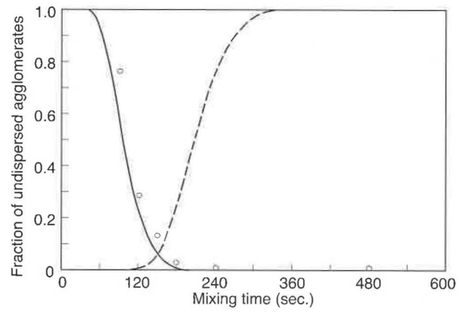

Figure 6.39 Fraction of undispersed carbon black, of size above 9 μm, as a function of mixing time inside a Banbury mixer. (O) denotes experimental results and solid line theoretical predictions. Broken line denotes the fraction of aggregates of size below 500 nm.

6.2.3.3 Mixing in Single Screw Extruders

Mixing caused by the cross-channel flow component can be further enhanced by introducing pins in the flow channel. These pins can either sit on the screw as shown in Fig. 6.40 [22] or on the barrel as shown in Fig. 6.41 [23]. The extruder with the adjustable pins on the barrel is generally referred to as QSM-extruder[6]. In both cases the pins disturb the flow by re-orienting the surfaces between fluids and by creating new surfaces by splitting the flow. Figure 6.42 presents a photograph of the channel contents of a QSM-extruder[7]. The photograph clearly demonstrates the re-orientation of the layers as the material flows past the pins. The pin type extruder is especially necessary for the mixing of high viscosity materials such as rubber compounds; thus, it is often called a cold feed rubber extruder. This machine is widely used in the production of rubber profiles of any shape and size.

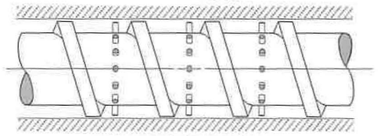

Figure 6.40 Pin mixing section on the screw of a single screw extruder.

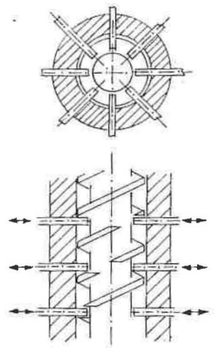

Figure 6.41 Pin barrel extruder (Quer Strom Misch Extruder).

6 QSM comes from the German *Quer Strom Misch* which translates into cross-flow mixing.
7 Courtesy of Paul Troester Maschinenfabrik, Hannover, Germany.

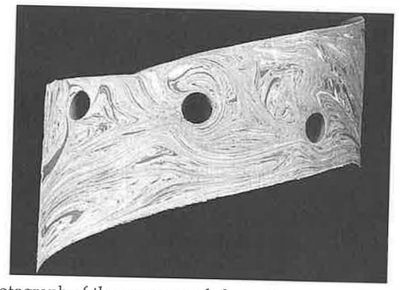

Figure 6.42 Photograph of the unwrapped channel contents of a pin barrel extruder.

For lower viscosity fluids, such as thermoplastic polymer melts, the mixing action caused by the cross-flow is often not sufficient to re-orient, distribute, and disperse the mixture, making it necessary to use special mixing sections. Re-orientation of the interfaces between primary and secondary fluids and distributive mixing can be induced by any disruption in the flow channel. Figure 6.43 [22] presents commonly used distributive mixing heads for single screw extruders. These mixing heads introduce several disruptions in the flow field which have proven to perform well in mixing.

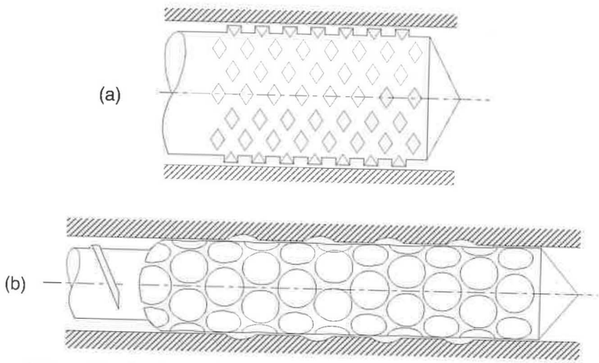

Figure 6.43 Distributive mixing sections: (a) Pineapple mixing section, (b) cavity transfer mixing section.

As mentioned earlier, dispersive mixing is required when breaking down particle agglomerates or when surface tension effects exist between primary and secondary fluids in the mixture. To disperse such systems, the mixture must be subjected to large stresses. Barrier-type screws are often sufficient to apply high stresses to the polymer melt. However, more intensive mixing can be applied by using a mixing head. When using barrier-type screws or a mixing head as shown in Fig. 6.44 [22] the mixture is forced through narrow gaps, causing high stresses in the melt. It should be noted that dispersive as well as distributive mixing heads result in a resistance to the flow, which results in viscous heating and pressure losses during extrusion.

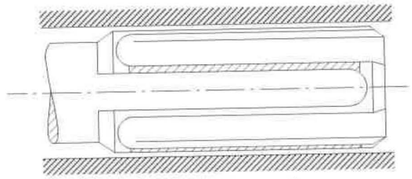

Figure 6.44 Maddock or Union Carbide mixing section.

6.2.3.4 Cokneader

The cokneader is a single screw extruder with pins on the barrel and a screw that oscillates in the axial direction. Figure 6.45 shows a schematic diagram of a cokneader. The pins on the barrel practically wipe the entire surface of the screw, making it the only self-cleaning single-screw extruder. This results in a reduced residence time, which makes it appropriate for processing thermally sensitive materials. The pins on the barrel also disrupt the solid bed creating a dispersed melting [24] which improves the overall melting rate while reducing the overall temperature in the material.

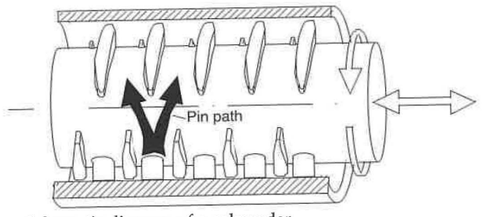

Figure 6.45 Schematic diagram of a cokneader.

A simplified analysis of a cokneader gives a number of striations per *L/D* of [25]

$$N_s = 2^{12} \tag{6.18}$$

which means that over a section of 4D the number of striations is $2^{12}(4) = 2.8E14$. A detailed discussion on the cokneader is given by Rauwendaal [25] and Elemans [26].

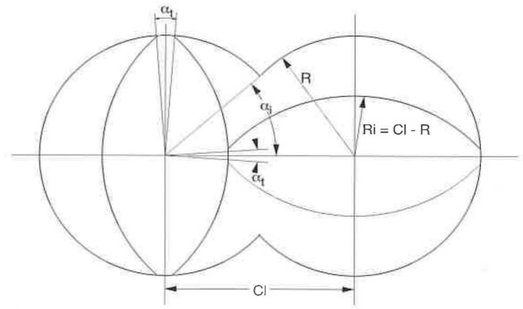

Figure 6.46 Geometry description of a double-flighted, co-rotating, self-cleaning, twin screw extruder.

6.2.3.5 Twin Screw Extruders

In the past two decades, twin screw extruders have developed into the best available continuous mixing devices. In general, they can be classified into intermeshing or non-intermeshing, and co-rotating or counter-rotating twin screw extruders[8]. The intermeshing twin screw extruders render a self-cleaning effect which evens-out the residence time of the polymer in the extruder. The self-cleaning geometry for a co-rotating double flighted twin screw extruder is shown in Fig. 6.46. The main characteristic of this type of configuration is that the surfaces of the screws are sliding past each other, constantly removing the polymer that is stuck to the screw.

In the last two decades, the co-rotating twin screw extruder systems have established themselves as efficient continuos mixers, including reactive extrusion. In essence, the co-rotating systems have a high pumping efficiency caused by the double transport action of the two screws. Counter- rotating

[8] A complete overview of twin screw extruders is given by White, J.L., *Twin Screw Extrusion-Technology and Principles*, Hanser Publishers, Munich, (1990).

systems generate high stresses because of the calendering action between the screws, making them efficient machines to disperse pigments and lubricants[9].

Several studies have been performed to evaluate the mixing capabilities of twin screw extruders. Noteworthy are two recent studies performed by Lim and White [27, 28] that evaluated the morphology development in a 30.7 mm diameter screw co-rotating [17] and a 34 mm diameter screw counter-rotating [18] intermeshing twin screw extruder. In both studies they dry-mixed 75/25 blend of polyethylene and polyamide 6 pellets that were fed into the hopper at 15 kg/h. Small samples were taken along the axis of the extruder and evaluated using optical and electron microscopy.

Figure 6.47 shows the morphology development along the screws at positions marked A, B, C, and D for a counter-rotating twin screw extruder configuration without special mixing elements. The dispersion of the blend becomes visible by the reduction of the characteristic size of the polyamide 6 phase. Figure 6.48 is a plot of the weight average and number average domain size of the polyamide 6 phase along the screw axis. The weight average phase size at the end of the extruder was measured to be 10 μm and the number average 6 μm. By replacing sections of the screw with one kneading-pump element and three special mixing elements, the final weight average phase size was reduced to 2.2 μm and the number average to 1.8 μm, as shown in Fig. 6.49.

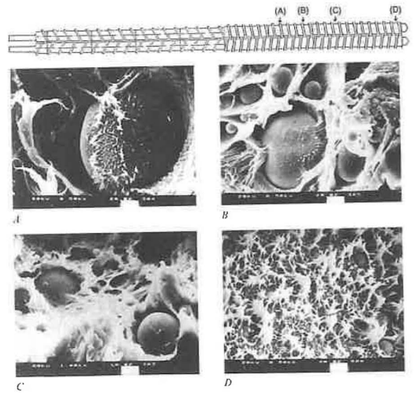

Figure 6.47 Morphology development inside a counter-rotating twin screw extruder.

9 There seems to be considerable disagreement about co- versus counter-rotating twin screw extruders between different groups in the polymer processing industry and academic community.

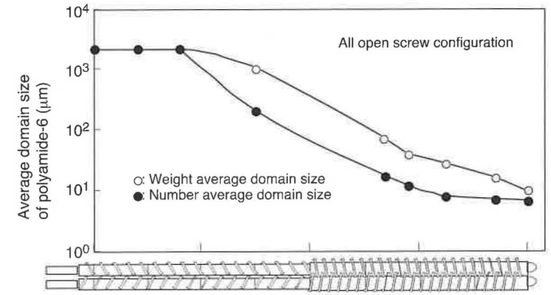

Figure 6.48 Number and weight average of polyamide 6 domain sizes along the screws for a counter-rotating twin screw extruder.

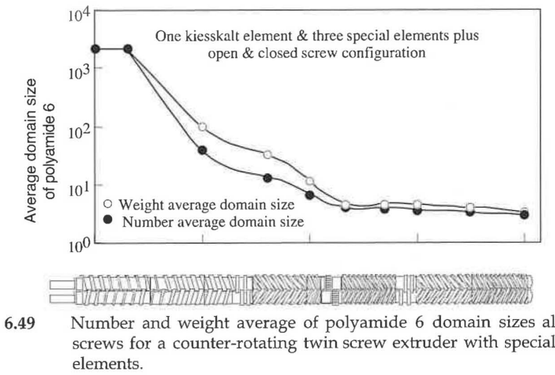

Figure 6.49 Number and weight average of polyamide 6 domain sizes along the screws for a counter-rotating twin screw extruder with special mixing elements.

Using a co-rotating twin screw extruder with three kneading disk blocks, a final morphology with polyamide 6 weight average phase sizes of 2.6 μm was achieved. Figure 6.50 shows the morphology development along the axis of the screws. When comparing the outcome of both counter-rotating (Fig. 6.49) and co-rotating (Fig. 6.50), it is clear that both extruders achieve a similar final mixing quality. However, the counter-rotating extruder achieved the final morphology much earlier in the screw than the co-rotating twin screw

extruder. A possible explanation for this is that the blend traveling through the counter-rotating configuration melted earlier than in the co-rotating geometry. In addition the phase size was slightly smaller, possibly due to the calendering effect between the screws in the counter-rotating system.

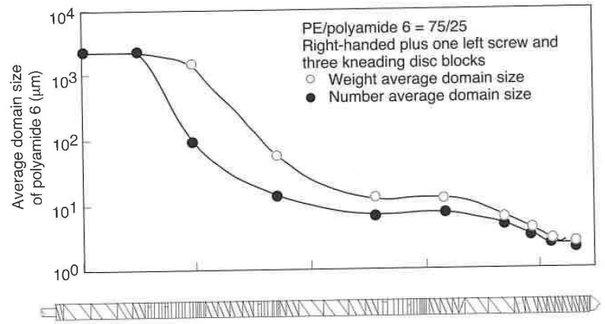

Figure 6.50 Number and weight average of polyamide 6 domain sizes along the screws for a co-rotating twin screw extruder with special mixing elements.

6.2.4 Energy Consumption During Mixing

Energy consumption is of extreme importance when assessing and comparing various mixing devices. High energy requirements for optimal mixing mean high costs and expensive equipment. The power consumption per unit volume of a deforming Newtonian fluid is given by [29]

$$p = 2\mu\left[\left(\frac{\partial v_x}{\partial x}\right)^2 + \left(\frac{\partial v_y}{\partial y}\right)^2 + \left(\frac{\partial v_z}{\partial z}\right)^2\right] + \mu\left[\left(\frac{\partial v_x}{\partial y} + \frac{\partial v_y}{\partial x}\right)^2 + \left(\frac{\partial v_y}{\partial z} + \frac{\partial v_z}{\partial y}\right)^2 + \left(\frac{\partial v_x}{\partial z} + \frac{\partial v_z}{\partial x}\right)^2\right] \quad (6.19)$$

Erwin [30] used the above equation to assess the energy input requirements for different types of mixing flows: simple shear, pure shear, and extensional flows. Table 6.4 presents flow fields and energy requirements for various flows described by Erwin [30]. For example, to produce a mixture such that $A/A_0 = 10^4$ in time $t_0 = 100$ s, for a fluid with viscosity $\mu = 10^4$ Pa – s, in a mixer which deforms the fluid with an elongational flow, one needs 96 kJ/m^3 of energy input. Since the flow is steady, this requires a power input of 0.96 kW/m^3 for 100 s. In a mixer that deforms the fluid in a biaxial extensional flow the energy

required is 24 kJ/m^3 with 0.24 kW/m^3 of power input. For the same amount of mixing, a mixer which deforms the fluid in pure shear requires an energy input of 40 kJ/m^3 or a steady power input of 0.4 kW/m^3 for 100 s. A device that deforms the fluid in simple shear requires a total energy input of 4x107 kJ/m^3 or a steady power input of 40,000 kW/m^3 for a 100 second period to achieve the same amount of mixing.

Table 6.4 Energy Input Requirements for Various Flow Mixers

Flow type	Flow field	Power	Energy input
Extensional flow (elongational)	$v_x = Gx$ $v_y = -Gy/2$ $v_z = -Gz/2$	$3\mu G^2$	$\frac{12\mu}{t_0}\left(\ln\left(\frac{5A}{4A_0}\right)\right)^2$
Extensional flow (biaxial)	$v_x = -Gx$ $v_y = Gy/2$ $v_z = Gz/2$	$3\mu G^2$	$\frac{3\mu}{t_0}\left(\ln\left(\frac{5A}{4A_0}\right)\right)^2$
Pure shear	$v_x = -hx$ $v_y = -Hy$ $v_z = 0$	$2\mu(h^2 + H^2)$	$\frac{4\mu}{t_0}\left(\ln\left(2\frac{A}{A_0}\right)\right)^2$
Simple shear	$v_x = -Gy$ $v_y = 0$ $v_z = 0$	μG^2	$\frac{4\mu}{t_0}\left(\frac{A}{A_0}\right)^2$

From this it is clear that, in terms of energy and power consumption, simple shear flows are significantly inferior to extensional flows.

6.2.5 Mixing Quality and Efficiency

In addition to the flow number, strain, and capillary number, several parameters have been developed by various researchers in the polymer industry to quantify the efficiency of the mixing processes. Some have used experimentally measured parameters while others have used mixing parameters which are easily calculated from computer simulation.

A parameter used in visual experiments is the batch homogenization time (BHT). This parameter is defined as the time it takes for a material to become homogeneously colored inside the mixing chamber after a small sample of colored pigment is placed near the center of the mixer. A downfall to this technique is that the observed homogenized time can be quite subjective.

To describe the state of the dispersion of fillers in a composite material, Suetsugu [31] used a dispersion index defined as:

$$\text{Dispersion index} = 1 - \phi_a \tag{6.20}$$

where ϕ_a is a dimensionless area that the agglomerates occupy and is defined by:

$$\phi_a = \frac{\pi}{4A\phi} \sum d_i^2 n_i \tag{6.21}$$

where A is the area under observation, ϕ the volume fraction of the filler, d_i the diameter of the agglomerate and n_i the number agglomerates. The dispersion index ranges between 0 for the worst case of dispersion and 1 where no agglomerates remain in the system.

A commonly used method to analyze the mixing capabilities of the extruder is the residence time distribution (RTD). It is calculated by monitoring the output of the extruder with the input of a secondary component. Two common response techniques are the step input response and the pulse input response shown in Fig. 6.51 [22]. The response of the input gives information on the mixing and conveying performance of the extruder. The RTD response to a pulse input for an ideal mixing situation is shown in Fig. 6.52. The figure shows a quick response to the input with a constant volume fraction of the secondary component until there is no material left.

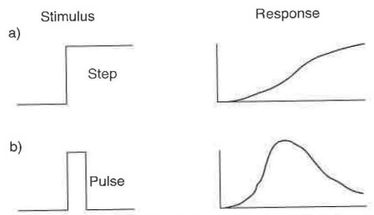

Figure 6.51 Step input and pulse input residence time distribution responses.

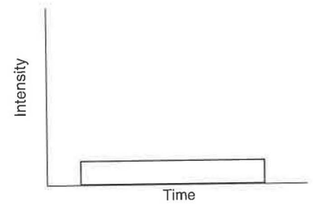

Figure 6.52 Ideal residence time distribution response to a pulse input.

By the use of a computer simulation, velocities, velocity gradients, and particle tracking can be computed with some degree of accuracy—depending on the computational method and assumptions made. Using information from a computer simulation, several methods to quantify mixing have been developed. Poincaré sections are often used to describe the particle paths during the mixing process. The Poincaré section shows the trajectory of several particles during the mixing process. They can be very useful in locating stagnation points, recirculation regions, and detecting symmetric flow patterns where no exchange exists across the planes of symmetry—all issues that hinder mixing.

6.2.6 Plasticization

Solvents, commonly referred to as plasticizers, are sometimes mixed into a polymer to dramatically alter its rheological and/or mechanical properties. Plasticizers are used as a processing aid since they have the same impact as raising the temperature of the material. Hence, the lowered viscosities at lower temperatures reduce the risk of thermal degradation during processing. For example, cellulose nitrite would thermally degrade during processing without the use of a plasticizer.

Plasticizers are more commonly used to alter a polymer's mechanical properties such as stiffness, toughness, and strength. For example, adding a plasticizer such as dioctylphthalate (DOP) to PVC can reduce its stiffness by three orders of magnitude and lower its glass transition temperature to -35 °C. In fact, a highly plasticized PVC is rubbery at room temperature. Table 6.5 [45] presents some common plasticizers with the polymers they plasticize, and their applications.

Since moisture is easily absorbed by polyamides, slightly modifying their mechanical behavior, it can be said that water acts as a plasticizing agent with these materials. Figure 6.53 shows the equilibrium water content for polyamide 6 and 66 as a function of the ambient relative humidity[10]. This moisture absorption causes the polyamide to expand or swell as shown in Fig. 6.54[11].

10 Courtesy of Bayer AG, Germany.
11 *Ibid.*

Table 6.5 Commercial Plasticizers and Their Applications

Plasticizer	Polymers	Plasticizer type
Di-octyl phthalate (DOP)	Polyvinyl chloride and copolymers	General purpose, primary plasticizer
Tricresyl phosphate (TCP)	Polyvinyl chloride and copolymers, cellulose acetate, cellulose nitrate	Flame retardant, primary plasticizer
Di-octyl adipate (DOA)	Polyvinyl chloride, cellulose acetate, butyrate	Low temperature plasticizer
Di-octyl sebacate (DOS)	Polyvinyl chloride , cellulose acetate, butyrate	Secondary plasticizer
Adipic acid polyesters (MW = 1500-3000)	Polyvinyl chloride	Non-migratory secondary plasticizer
Sebacic acid polyesters (MW = 1500-3000)	Polyvinyl chloride	Non-migratory secondary plasticizer
Chlorinated paraffins (%CI = 40-70) (MW = 600-1000)	Most polymers	Flame retardant, plasticizer extenders
Bi- and terphenyls (also hydrogenated)	Aromatic polyesters	Various
N-ethyl-toluene sulphonamide	Polyamides	General purpose, primary plasticizer
Sulphonamide-formaldehyde resins	Polyamides	Non-migratory secondary plasticizers

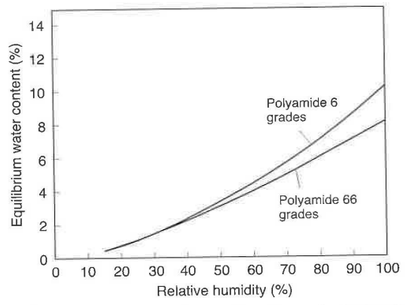

Figure 6.53 Equilibrium water content as a function of relative humidity for polyamide 6 and polyamide 66.

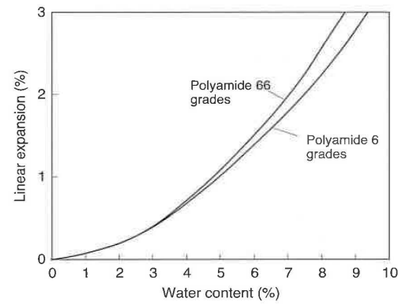

Figure 6.54 Linear expansion as a function of water content for polyamide 6 and polyamide 66.

The behavior of polymers toward solvents depends in great part on the nature of the solvent and on the structure of the polymer molecules. If the basic building block of the macromolecule and the solvent molecule are the same or of similar nature, then the absorption of a solution will lead to swelling. If a sufficient amount is added, the polymer will dissolve in the solvent. Crystalline regions of a semi-crystalline thermoplastic are usually not affected by solvents, whereas amorphous regions are easily penetrated. In addition, the degree of cross-linking in thermosets and elastomers has a great influence on whether a material can be permeated by solvents. The shorter the distances between the linked molecules, the less solvent molecules can permeate and give mobility to chain segments. While elastomers can swell in the presence of a solvent, highly cross-linked thermosets do not swell or dissolve.

The amount of solvent that is absorbed depends not only on the chemical structure of the two materials but also on the temperature. Since an increase in temperature reduces the covalent forces of the polymer, solubility becomes higher. Although it is difficult to determine the solubility of polymers, there are some rules to estimate it. The simplest rule is: same dissolves same (i.e., when both—polymer and solvent--have the same valence forces, solubility exists).

The solubility of a polymer and a solvent can be addressed from a thermodynamic point of view using the familiar Gibbs free energy equation

$$\Delta G = \Delta H - T\Delta S \tag{6.22}$$

where ΔG is the change in free energy, ΔH is the change in enthalpy, ΔS the change in entropy and T the temperature. If ΔG in Eq. 6.22 is negative

solubility, is possible. A positive ΔH suggests that polymer and the solvent do not "want" to mix, which means solubility can only occur if $\Delta H < T\,\Delta S$. On the other hand, $\Delta H \approx 0$ implies that solubility is the natural lower energy state. Since the entropy change when dissolving a polymer is very small, the determining factor if a solution will occur or not is the change in enthalpy, ΔH. Hildebrand and Scott [46] proposed a useful equation that estimates the change in enthalpy during the formation of a solution. The Hildebrand equation is stated by

$$\Delta H = V\left(\left(\frac{\Delta E_1}{V_1}\right)^{1/2} - \left(\frac{\Delta E_2}{V_2}\right)^{1/2}\right)^2 \phi_1\phi_2 \tag{6.23}$$

where V is the total volume of the mixture, V_1 and V_2 the volumes of the solvent and polymer, ΔE_1 and ΔE_2 their energy of evaporation and, ϕ_1 and ϕ_2 their volume fractions. Equation 6.23 can be simplified to

$$\Delta H = V(\delta_1 - \delta_2)^2 \phi_1\phi_2 \tag{6.24}$$

where δ is called the solubility parameter and is defined by

$$\delta = \left(\frac{\Delta E}{V}\right)^{1/2} \tag{6.25}$$

If the solubility parameter of the substances are nearly equal they will dissolve. A rule-of-thumb can be used that if $|\delta_1 - \delta_2| < 1$ $(\text{cal/cm}^3)^{1/2}$ solubility will occur [47]. The units $(\text{cal/cm}^3)^{1/2}$ are usually referred to as Hildebrands. Solubility parameters for various polymers are presented in Table 6.6 [48], and for various solvents in Table 6.7 [48].

Figure 6.55 [49] shows a schematic diagram of swelling and dissolving behavior of cross-linked and uncross-linked polymers as a function of the solubility or *solubility parameter*, δ_s, of the solvent. When the solubility parameter of the polymer and the solvent approach each other, the uncross-linked polymer becomes unconditionally soluble. However, if the same polymer is cross-linked then it is only capable of swelling. The amount of swelling depends on the degree of cross-linking.

Table 6.6 Solubility Parameter for Various Polymers

Polymer	$\delta\left(\text{cal/cm}^3\right)^{1/2}$
Polytetrafluoroethylene	6.2
Polyethylene	7.9
Polypropylene	8.0
Polyisobutylene	8.1
Polyisoprene	8.3
Polybutadiene	8.6
Polystyrene	9.1
Poly(vinyl acetate)	9.4
Poly(methyl methacrylate)	9.5
Polycarbonate	9.9
Polysulphone	9.9
Poly(vinyl chloride)	10.1
Polyethylene terephthalate	10.2
Polyamide 6	11.0
Cellulose nitrate	11.5
Poly(vinylidene chloride)	12.2
Polyamide 66	13.6
Polyacrylonitrile	15.4

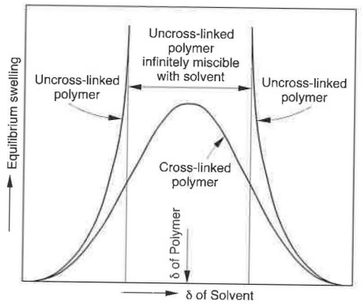

Figure 6.55 Equilibrium swelling as a function of solubility parameter for cross-linked and uncross-linked polymers.

Table 6.7 Solubility Parameter of Various Plasticizers and Solvents

Solvent	$\delta\left(\text{cal}/\text{cm}^3\right)^{1/2}$
Acetone	10.0
Benzene	9.1
Di-butoxyethyl phthalate (Dronisol)	8.0
n-butyl alcohol	11.4
Sec-butyl alcohol	10.8
Butyl stearate	7.5
Chlorobenzene	9.6
Cyclohexanone	9.9
Dibutyl phenyl phosphate	8.7
Dibutyl phthalate	9.3
Dibutyl sebacate	9.2
Diethyl phthalate	10.0
Di-n-hexyl phthalate	8.9
Diisodecyl phthalate	7.2
Dimethyl phthalate	10.7
Dioctyl adipate	8.7
Dioctyl phthalate (DOP)	7.9
Dioctyl sebacate	8.6
Dipropyl phthalate	9.7
Ethyl acetate	9.1
Ethyl alcohol	12.7
Ethylene glycol	14.2
2-ethylhexyl diphenyl phosphate (Santicizer 141)	8.4
N-ethyl-toluenesulfonamide (Santicizer 8)	11.9
Hydrogenated terphenyl (HB-40)	9.0
Kronisol	8.0
Methanol	14.5
Methyl ethyl ketone	9.3
Nitromethane	12.7
n-propyl alcohol	11.9
Toluene	8.9
Tributyl phophate	8.2
1,1,2-trichloro-1,2,2-trifluoroethane (freon 113)	7.2
Trichloromethane (chloroform)	9.2
Tricresyl phosphate	9.0
Triphenyl phosphate	9.2
Water	23.4
Xylene	8.8

6.3 Injection Molding

Injection molding is the most important process used to manufacture plastic products. Today, more than one-third of all thermoplastic materials are injection molded and more than half of all polymer processing equipment is for injection molding. The injection molding process is ideally suited to manufacture mass-produced parts of complex shapes requiring precise dimensions. The process goes back to 1872 when the Hyatt brothers patented their stuffing machine to inject cellulose into molds. However, today's injection molding machines are mainly related to the reciprocating screw injection molding machine patented in 1956. A modern injection molding machine with its most important elements is shown in Fig. 6.56. The components of the injection molding machine are the plasticating unit, clamping unit, and the mold.

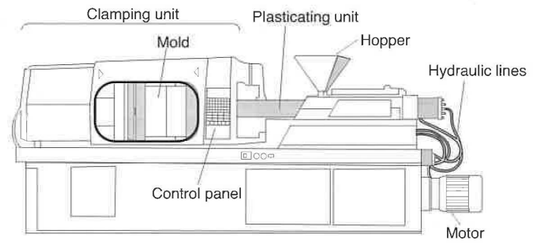

Figure 6.56 Schematic of an injection molding machine.

Today, injection molding machines are classified by the following international convention[12]

Manufacturer T / P

where T is the clamping force in metric tons and P is defined as

$$P = \frac{V_{\max} p_{\max}}{1000} \tag{6.26}$$

where $V_{\max}$ is the maximum shot size in cm3 and $p_{\max}$ is the maximum injection pressure in bar. The clamping forced T can be as low as 1 metric ton for small machines, and as high as 11,000 tons.

12 The old US convention uses MANUFACTURER T-v where T is the clamping force in British tons and v the shot size in ounces of polystyrene.

6.3.1 The Injection Molding Cycle

The sequence of events during the injection molding of a plastic part, as shown in Fig. 6.57, is called the injection molding cycle. The cycle begins when the mold closes, followed by the injection of the polymer into the mold cavity. Once the cavity is filled, a holding pressure is maintained to compensate for material shrinkage. In the next step, the screw turns, feeding the next shot to the front of the screw. This causes the screw to retract as the next shot is prepared. Once the part is sufficiently cool, the mold opens and the part is ejected.

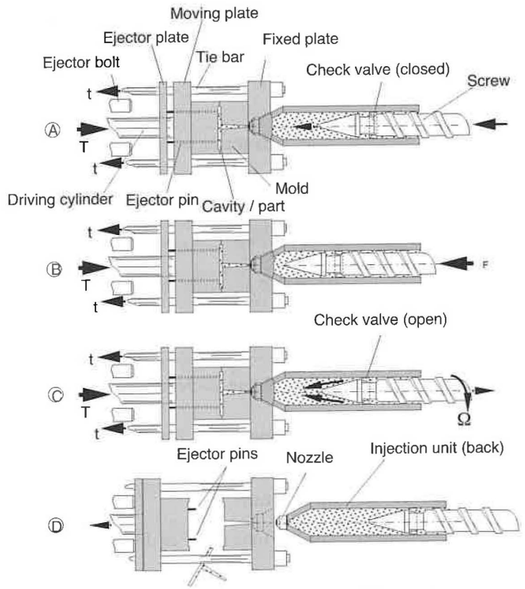

Figure 6.57 Sequence of events during an injection molding cycle.

Figure 6.58 presents the sequence of events during the injection molding cycle. The figure shows that the cycle time is dominated by the cooling of the part inside the mold cavity. The total cycle time can be calculated using

$$t_{cycle} = t_{closing} + t_{cooling} + t_{ejection} \tag{6.27}$$

where the closing and ejection times, $t_{closing}$ and $t_{ejection}$, can last from a fraction of second to a few seconds, depending on the size of the mold and machine. The cooling times, which dominate the process, depend on the maximum thickness of the part. The cooling time for a plate-like part of thickness h can be estimated using

$$t_{cooling} = \frac{h^2}{\pi\alpha}\ln\left(\frac{8}{\pi^2}\frac{T_m - T_w}{T_D - T_w}\right) \tag{6.28}$$

and for a cylindrical geometry of diameter D using

$$t_{cooling} = \frac{D^2}{23.14\alpha}\ln\left(0.692\frac{T_m - T_w}{T_D - T_w}\right) \tag{6.29}$$

where T_m represents the temperature of the injected melt, T_w the temperature of the mold wall, T_D the average temperature at ejection, and α the thermal diffusivity.

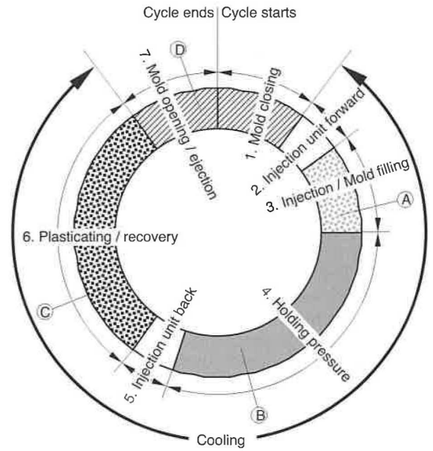

Figure 6.58 Injection molding cycle.

Using the average part temperature history and the cavity pressure history, the process can be followed and assessed using the PvT diagram as depicted in Fig. 6.59 [32-33]. To follow the process on the PvT diagram, we must transfer both the temperature and the pressure at matching times. The diagram reveals four basic processes: an isothermal injection (0-1) with pressure rising to the holding pressure (1-2), an isobaric cooling process during the holding cycle (2-3), an isochoric cooling after the gate freezes with a pressure drop to atmospheric (3-4), and then isobaric cooling to room temperature (4-5).

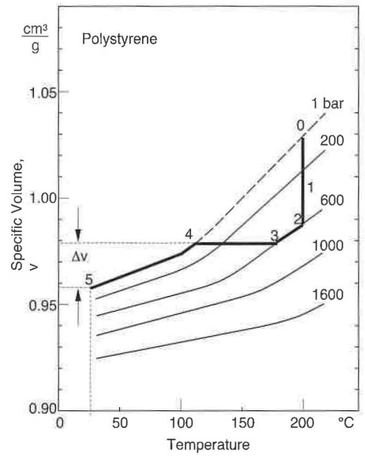

Figure 6.59 Trace of an injection molding cycle in a PvT diagram.

The point on the PvT diagram where the final isobaric cooling begins (4), controls the total part shrinkage, Δv. This point is influenced by the two main processing conditions - the melt temperature, T_m, and the holding pressure, P_H, as depicted in Fig. 6.60. Here the process in Fig. 6.59 is compared to one with a higher holding pressure. Of course, there is an infinite combination of conditions that render acceptable parts, bound by minimum and maximum temperatures and pressures. Figure 6.61 presents the molding diagram with all limiting conditions. The melt temperature is bound by a low temperature that results in a short shot or unfilled cavity and a high temperature that leads to material degradation. The hold pressure is bound by a low pressure that leads to excessive shrinkage or low part weight, and a high pressure that results in

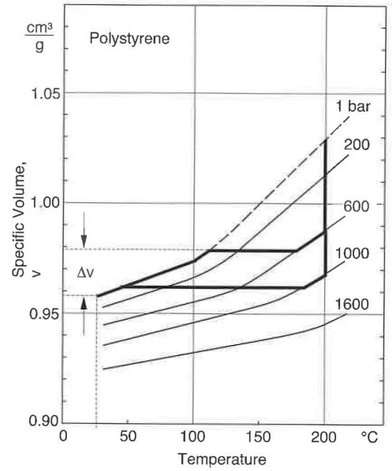

Figure 6.60 Trace of two different injection molding cycles in a PvT diagram.

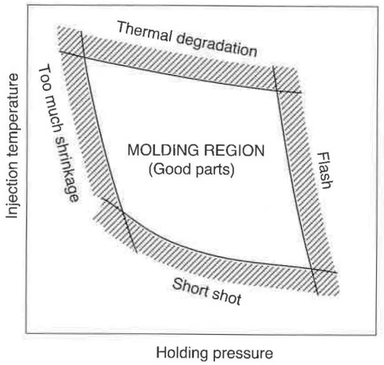

Figure 6.61 The molding diagram.

flash. Flash results when the cavity pressure force exceeds the machine clamping force, leading to melt flow across the mold parting line. The holding pressure determines the corresponding clamping force required to size the injection molding machine. An experienced polymer processing engineer can usually determine which injection molding machine is appropriate for a specific application. For the untrained polymer processing engineer, finding this appropriate holding pressure and its corresponding mold clamping force can be difficult.

With difficulty one can control and predict the component's shape and residual stresses at room temperature. For example, sink marks in the final product are caused by material shrinkage during cooling, and residual stresses can lead to environmental stress cracking under certain conditions [35].

Warpage in the final product is often caused by processing conditions that lead to asymmetric residual stress distributions through the part thickness. The formation of residual stresses in injection molded parts is attributed to two major coupled factors: cooling and flow stresses. The first and most important is the residual stress formed as a result of rapid cooling which leads to large temperature variations.

6.3.2 The Injection Molding Machine

6.3.2.1 The Plasticating and Injection Unit

A plasticating and injection unit is shown in Fig. 6.62. The major tasks of the plasticating unit are to melt the polymer, to accumulate the melt in the screw chamber, to inject the melt into the cavity, and to maintain the holding pressure during cooling.

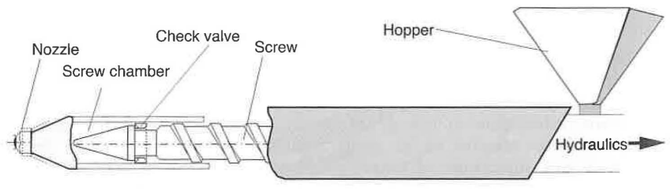

Figure 6.62 Schematic of the plasticating unit.

The main elements of the plasticating unit follow:

- Hopper
- Screw
- Heater bands
- Check valve
- Nozzle

The hopper, heating bands, and the screw are similar to a plasticating single screw extruder, except that the screw in an injection molding machine can slide back and forth to allow for melt accumulation and injection. This characteristic gives it the name reciprocating screw. For qquality purposes, the maximum stroke in a reciprocating screw should be set smaller than 3D.

Although the most common screw used in injection molding machines is the three-zone plasticating screw, two stage vented screws are often used to extract moisture and monomer gases just after the melting stage.

The check valve, or non-return valve, is at the end of the screw and enables it to work as a plunger during injection and packing without allowing polymer melt back flow into the screw channel. A check valve and its function during operation is depicted in Fig. 6.57, and in Fig. 6.62. A high quality check valve allows less then 5% of the melt back into the screw channel during injection and packing.

The nozzle is at the end of the plasticating unit and fits tightly against the sprue bushing during injection. The nozzle type is either open or shut-off. The open nozzle is the simplest, rendering the lowest pressure consumption.

6.3.2.2 The Clamping Unit

The job of a clamping unit in an injection molding machine is to open and close the mold, and to close the mold tightly to avoid flash during the filling and holding. Modern injection molding machines have two predominant clamping types: mechanical and hydraulic.

Figure 6.63 presents a toggle mechanism in the open and closed mold positions. Although the toggle is essentially a mechanical device, it is actuated by a hydraulic cylinder. The advantage of using a toggle mechanism is that, as the mold approaches closure, the available closing force increases and the closing decelerates significantly. However, the toggle mechanism only transmits its maximum closing force when the system is fully extended.

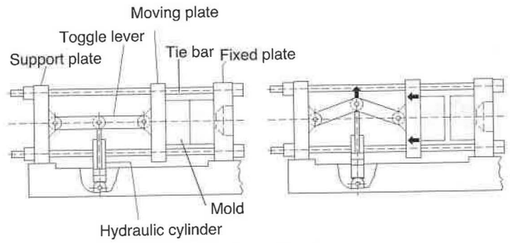

Figure 6.63 Clamping unit with a toggle mechanism.

Figure 6.64 presents a schematic of a hydraulic clamping unit in the open and closed positions. The advantages of the hydraulic system is that a maximum clamping force is attained at any mold closing position and that the system can take different mold sizes without major system adjustments.

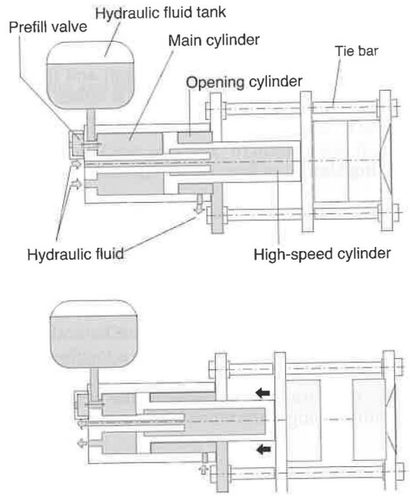

Figure 6.64 Hydraulic clamping unit.

6.3.2.3 The Mold Cavity

The central point in an injection molding machine is the mold. The mold distributes polymer melt into and throughout the cavities, shapes the part, cools the melt and, ejects the finished product. As depicted in Fig. 6.65, the mold is custom-made and consists of the following elements:

- Sprue and runner system
- Gate
- Mold cavity
- Cooling system (thermoplastics)
- Ejector system

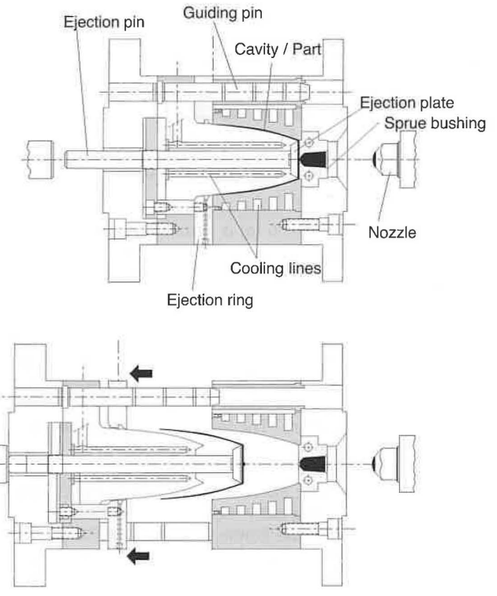

Figure 6.65 An injection mold.

During mold filling, the melt flows through the sprue and is distributed into the cavities by the runners, as seen in Fig. 6.66.

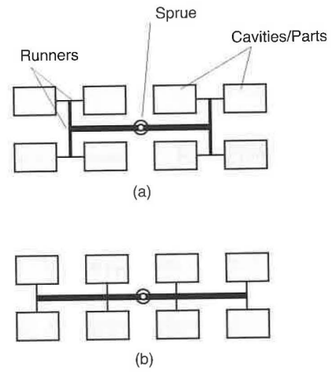

Figure 6.66 Schematic of different runner system arrangements.

The runner system in Fig. 6.66 (a) is symmetric where all cavities fill at the same time causing the polymer to fill all cavities in the same way. The disadvantage of this balanced runner system is that the flow paths are long, leading to high material and pressure consumption. On the other hand, the asymmetric runner system shown in Fig. 6.66 (b) leads to parts of different quality. Equal filling of the mold cavities can also be achieved by varying runner diameters. There are two types of runner systems - cold and hot. Cold runners are ejected with the part, and are trimmed after mold removal. The advantage of the cold runner is lower mold cost. The hot runner keeps the polymer at its melt temperature. The material stays in the runner system after ejection, and is injected into the cavity in the following cycle. There are two types of hot runner system: externally and internally heated. The externally heated runners have a heating element surrounding the runner that keeps the polymer isothermal. The internally heated runners have a heating element running along the center of the runner, maintaining a polymer melt that is warmer at its center and possibly solidified along the outer runner surface. Although a hot runner system considerably increases mold cost, its advantages include elimination of trim and lower pressures for injection.

When large items are injection molded, the sprue sometimes serves as the gate, as shown in Fig. 6.67. The sprue must be subsequently trimmed, often

requiring further surface finishing. On the other hand, a pin-type gate (Fig. 6.67) is a small orifice that connects the sprue or the runners to the mold cavity. The part is easily broken off from such a gate, leaving only a small mark that usually does not require finishing. Other types of gates, also shown in Fig. 6.67, are film gates, used to eliminate orientation, and disk or diaphragm gates for symmetric parts such as compact discs.

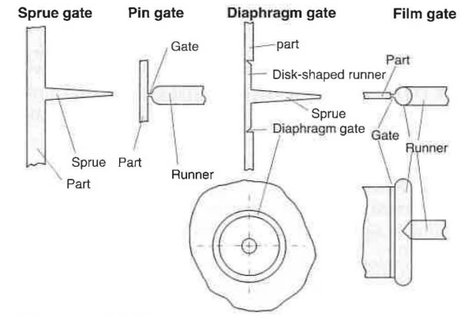

Figure 6.67 Schematic of different gating systems.

6.3.3 Related Injection Molding Processes

Although most injection molding processes are covered by the conventional process description discussed earlier in this chapter, there are several important molding variations including:

- Multi-color
- Multi-component
- Co-injection
- Gas-assisted
- Injection-compression

Multi-component injection molding occurs when two or more polymers, or equal polymers of different color, are injected through different runner and gate systems at different stages during the molding process. Each component is injected using its own plasticating unit. The molds are often located on a turntable. Multi-color automotive stop lights are molded this way.

In principle, the multi-component injection molding process is the same as the multi-color process. Here, either two incompatible materials are molded or

one component is cooled sufficiently so that the two components do not adhere to each other. For example, to mold a ball and socket system, the socket of the linkage is molded first. The socket component is allowed to cool somewhat and the ball part is injected inside it. This results in a perfectly movable system. This type of injection molding process is used to replace tedious assembling tasks and is becoming popular in countries where labor costs are high. In addition, today, a widely used application is the multi-component injection of a hard and a soft polymer such as polypropylene with a thermoplastic elastomer.

In contrast to multi-color and multi-component injection molding, co-injection molding uses the same gate and runner system. Here, the component that ends as the outer skin of the part is injected first, followed by the core component. The core component displaces the first and a combination of the no-slip condition between polymer and mold and the freezing of the melt creates a sandwiched structure as depicted in Fig. 6.68.

In principle, the gas-assisted injection molding process is similar to co-injection molding. Here, the second or core component is nitrogen, which is injected through a needle into the polymer melt, blowing the melt out of the way and depositing it against the mold surfaces.

Injection-compression molding first injects the material into a partially opened mold, and then squeezes the material by closing the mold. Injection-compression molding is used for polymer products that require a high quality surface finish, such as compact discs and other optically demanding components because it practically eliminates tangential molecular orientation.

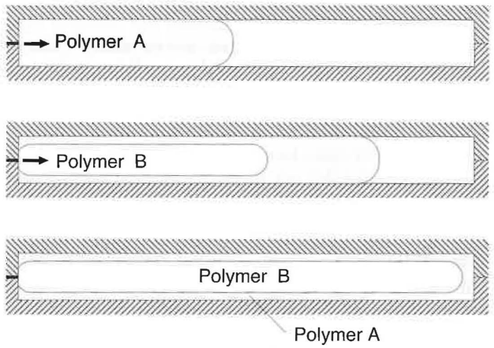

Figure 6.68 Schematic of the co-injection molding process.

6.4 Secondary Shaping

Secondary shaping operations such as extrusion blow molding, film blowing, and fiber spinning occur immediately after the extrusion profile emerges from the die. The thermoforming process is performed on sheets or plates previously extruded and solidified. In general, secondary shaping operations consist of mechanical stretching or forming of a preformed cylinder, sheet, or membrane.

6.4.1 Fiber Spinning

Fiber spinning is used to manufacture synthetic fibers. During fiber spinning, a filament is continuously extruded through an orifice and stretched to diameters of 100 μm and smaller. The process is schematically depicted in Fig. 6.69. The molten polymer is first extruded through a filter or *screen pack*, to eliminate small contaminants. The melt is then extruded through a spinneret, a die composed of multiple orifices. A spinneret can have between one and 10,000 holes. The fibers are then drawn to their final diameter, solidified, and wound onto a spool. The solidification takes place either in a water bath or by forced convection. When the fiber solidifies in a water bath, the extrudate undergoes an adiabatic stretch before cooling begins in the bath. The forced convection cooling, which is more commonly used, leads to a non-isothermal spinning process.

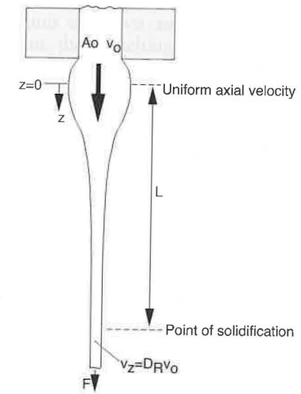

Figure 6.69 The fiber spinning process.

The drawing and cooling processes determine the morphology and mechanical properties of the final fiber. For example, ultra high molecular weight HDPE fibers with high degrees of orientation in the axial direction can have the stiffness of steel with today's fiber spinning technology.

Of major concern during fiber spinning are the instabilities that arise during drawing, such as brittle fracture, Rayleigh disturbances, and draw resonance. Brittle fracture occurs when the elongational stress exceeds the melt strength of the drawn polymer melt. The instabilities caused by Rayleigh disturbances are like those causing filament break-up during dispersive mixing as discussed in Chapter 5. Draw resonance appears under certain conditions and manifests itself as periodic fluctuations that result in diameter oscillation.

6.4.2 Film Production

6.4.2.1 Cast Film Extrusion

In a cast film extrusion process, a thin film is extruded through a slit onto a chilled, highly polished, turning roll where it is quenched from one side. The speed of the roller controls the draw ratio and final film thickness. The film is then sent to a second roller for cooling of the other side. Finally, the film passes through a system of rollers and is wound onto a roll. A typical film casting process is depicted in Fig. 6.70 and 6.71. The cast film extrusion process exhibits stability problems similar to those encountered in fiber spinning [36].

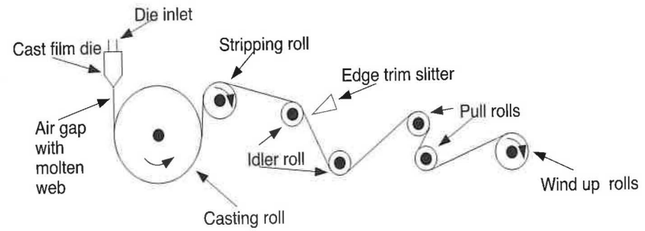

Figure 6.70 Schematic of a film casting operation.

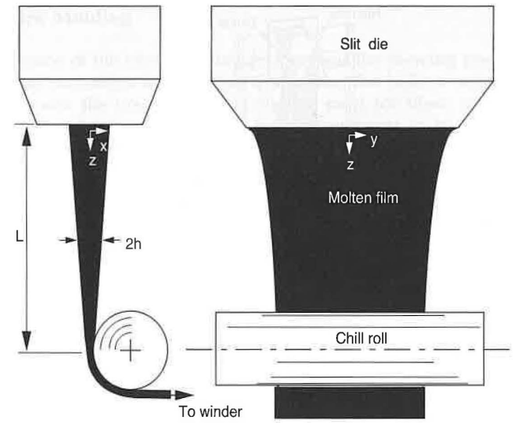

Figure 6.71 Film casting.

6.4.2.2 Film Blowing

In film blowing, a tubular cross-section is extruded through an annular die, normally a spiral die, and is drawn and inflated until the freezing line is reached. Beyond this point, the stretching is practically negligible. The process is schematically depicted in Fig. 6.72 [37] and Fig. 6.73. The advantage of film blowing over casting is that the induced biaxial stretching renders a stronger and less permeable film. Film blowing is mainly used with less expensive materials such as polyolefins. Polymers with lower viscosity such as PA and PET are better manufactured using the cast film process.

The extruded tubular profile passes through one or two air rings to cool the material. The tube interior is maintained at a certain pressure by blowing air into the tube through a small orifice in the die mandrel. The air is retained in the tubular film, or bubble, by collapsing the film well above its freeze-off point and tightly pinching it between rollers. The size of the tubular film is calibrated between the air ring and the collapsing rolls.

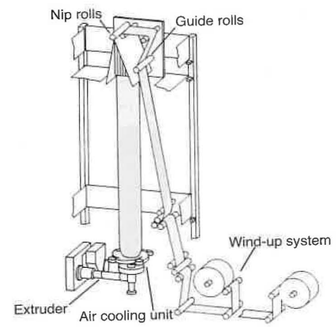

Figure 6.72 Film blowing.

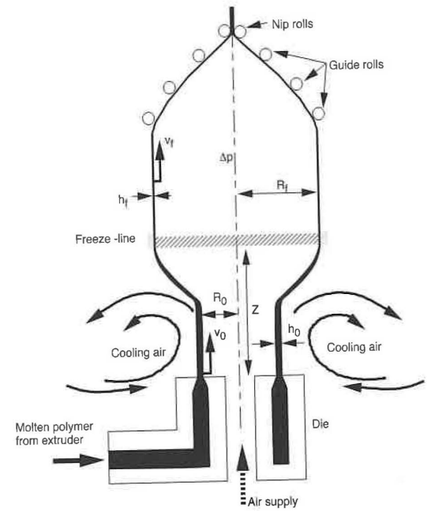

Figure 6.73 Film blowing.

6.4.3 Blow Molding

The predecessor of the blow molding process was the blowing press developed by Hyatt and Burroughs in the 1860s to manufacture hollow celluloid articles. Polystyrene was the first synthetic polymer used for blow molding during World War II and polyethylene was the first material to be implemented in commercial applications. Until the late 1950s, the main application for blow molding was the manufacture of LDPE articles such as squeeze bottles.

Blow molding produces hollow articles that do not require a homogeneous thickness distribution. Today, HDPE, LDPE, PP, PET, and PVC are the most common materials used for blow molding.

6.4.3.1 Extrusion Blow Molding

In extrusion blow molding, a *parison* or tubular profile is extruded and inflated into a cavity with the specified geometry. The blown article is held inside the cavity until it is sufficiently cool. Figure 6.74 [38] presents a schematic of the steps in blow molding.

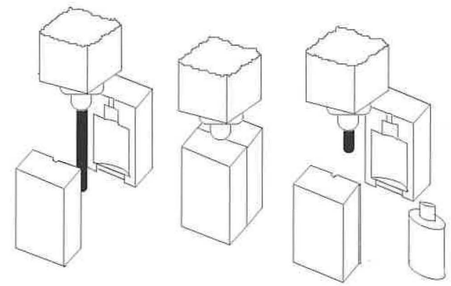

Figure 6.74 Schematic of the extrusion blow molding process.

During blow molding, one must generate the appropriate parison length such that the trim material is minimized. Another means of saving material is generating a parison of variable thickness, usually referred to as *parison programming*, such that an article with an evenly distributed wall thickness is achieved after stretching the material. An example of a programmed parison and finished bottle thickness distribution is presented in Fig. 6.75 [39].

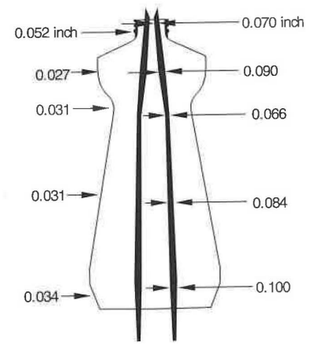

Figure 6.75 Wall thickness distribution in the parison and the part.

A parison of variable thickness can be generated by moving the mandrel vertically during extrusion as shown in Fig. 6.76. A thinner wall not only results in material savings but also reduces the cycle time due to the shorter required cooling times.

As expected, the largest portion of the cycle time is the cooling of the blow molded container in the mold cavity. Most machines wor with multiple molds in order to increase production. Rotary molds are often used in conjunction with vertical or horizontal rotating tables (Fig. 6.77 [37]).

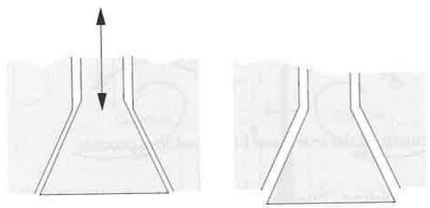

Figure 6.76 Moving mandrel used to generate a programmed parison.

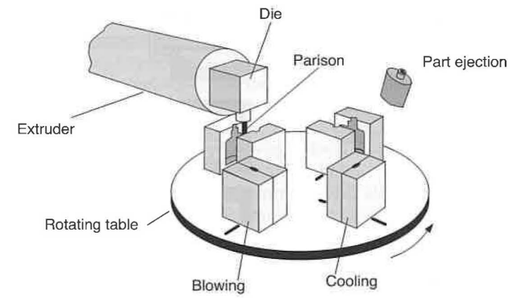

Figure 6.77 Schematic of an extrusion blow molder with a rotating table.

6.4.3.2 Injection Blow Molding

Injection blow molding depicted in Fig. 6.78 [38] begins by injection molding the parison onto a core and into a mold with finished bottle threads. The formed parison has a thickness distribution that leads to reduced thickness variations throughout the container. Before blowing the parison into the cavity, it can be mechanically stretched to orient molecules axially, Fig. 6.79 [38]. The subsequent blowing operation introduces tangential orientation. A container with biaxial molecular orientation exhibits higher optical (clarity) and mechanical properties and lower permeability. In the injection blow molding process one can go directly from injection to blowing or one can have a re-heating stage in-between.

The advantages of injection blow molding over extrusion blow molding are:

- Pinch-off and therefore post-mold trimming are eliminated
- Controlled container wall thickness
- Dimensional control of the neck and screw-top of bottles and containers

Disadvantages include higher initial mold cost, the need for both injection and blow molding units and lower volume production.

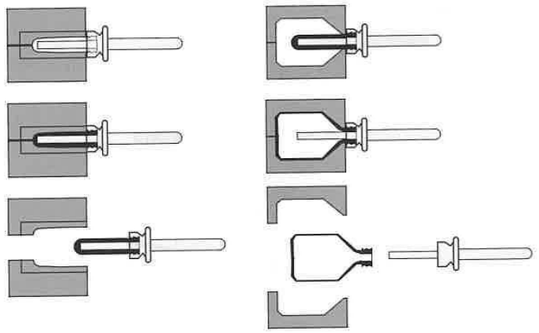

Figure 6.78 Injection blow molding.

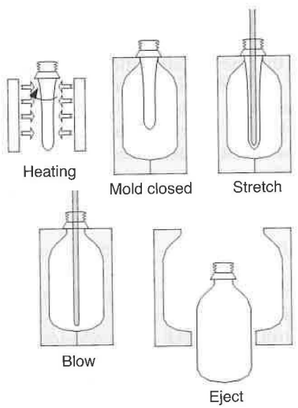

Figure 6.79 Stretch blow molding.

6.4.3.3 Thermoforming

Thermoforming is an important secondary shaping method of plastic film and sheet. Thermoforming consists of warming the plastic sheet and forming it into a cavity or over a tool using vacuum, air pressure, and mechanical means. During the 18th century, tortoiseshells and hooves were thermoformed into combs and other shapes. The process was refined during the mid-19th century to thermoform various cellulose nitrate articles. During World War II, thermoforming was used to manufacture acrylic aircraft cockpit enclosures, canopies, and windshields, as well as translucent covers for outdoor neon signs. During the 1950s, the process made an impact in the mass production of cups, blister packs, and other packaging commodities. Today, in addition to packaging, thermoforming is used to manufacture refrigerator liners, pick-up truck cargo box liners, shower stalls, bathtubs, as well as automotive trunk liners, glove compartments, and door panels.

A typical thermoforming process is presented in Fig. 6.80 [37]. The process begins by heating the plastic sheet slightly above the glass transition temperature, for amorphous polymers, or slightly below the melting point, for semi-crystalline materials. Although, both amorphous and semi-crystalline polymers are used for thermoforming, the process is easiest with amorphous polymers because they have a wide rubbery temperature range above the glass transition temperature. At these temperatures the polymer is easily shaped, but still has enough rigidity to hold the heated sheet without much sagging. Most semi-crystalline polymers lose their strength rapidly once the crystalline structure breaks up above the melting temperature.

The heating is achieved using radiative heaters and the temperature reached during heating must be high enough for sheet shaping, but low enough so the sheets do not droop into the heaters. One key requirement for successful thermoforming is to bring the sheet to a uniform forming temperature. The sheet is then shaped into the cavity over the tool. This can be accomplished in several ways. Most commonly a vacuum sucks the sheet onto the tool, stretching the sheet until it contacts the tool surface. The main problem here is the irregular thickness distribution that arises throughout the part. Hence, the main concern of the process engineer is to optimize the system such that the differences in thickness throughout the part are minimized. This can be accomplished in many ways but most commonly by plug-assist. Here, as the plug pushes the sheet into the cavity, only the parts of the sheet not touching the plug-assist stretch. Since the unstretched portions of the sheet must remain hot for subsequent stretching, the plug-assist is made of a low thermal conductivity material such as wood or hard rubber. The initial stretch is followed by a vacuum for final shaping. Once cooled, the product is removed.

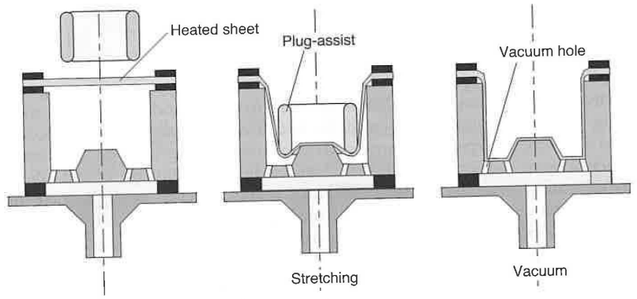

Figure 6.80 Plug-assist thermoforming using vacuum.

To reduce thickness variations in the product, the sheet can be pre stretched by forming a bubble at the beginning of the process. This is schematically depicted in Fig. 6.81 [37]. The mold is raised into the bubble, or a plug-assist pushes the bubble into the cavity, and a vacuum finishes the process.

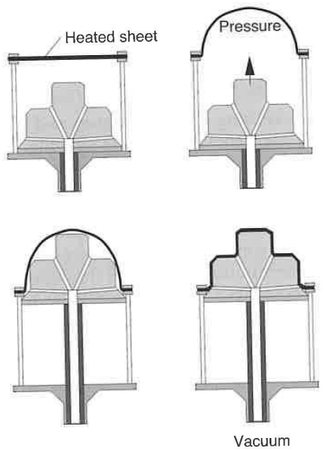

Figure 6.81 Reverse draw thermoforming with plug-assist and vacuum.

One of the main reasons for the rapid growth and high volume of thermoformed products is that the tooling costs for a thermoforming mold are much lower than for injection molding.

6.5 Calendering

In a calender line, the polymer melt is transformed into films and sheets by squeezing it between pairs of co-rotating high precision rollers. Calenders are also used to produce certain surface textures which may be required for different applications. Today, calendering lines are used to manufacture PVC sheet, floor covering, rubber sheet, and rubber tires. They are also used to texture or emboss surfaces. When producing PVC sheet and film, calender lines have a great advantage over extrusion processes because of the shorter residence times, resulting in a lower requirement for stabilizer. This can be cost effective since stabilizers are a major part of the overall expense of processing these polymers.

Figure 6.82 [37] presents a typical calender line for manufacturing PVC sheet. A typical system is composed of:

- Plasticating unit
- Calender
- Cooling unit
- Accumulator
- Wind-up station

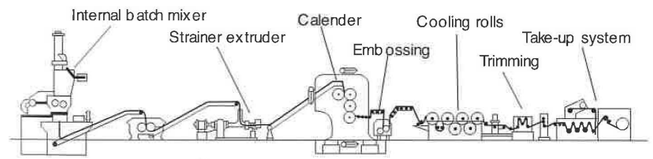

Figure 6.82 Schematic of a typical calendering process (Berstorff GmbH).

In the plasticating unit, which is represented by the internal batch mixer and the strainer extruder, the material is melted and mixed and is fed in a continuous stream between the nip of the first two rolls. In another variation of the process, the mixing may take place elsewhere, and the material is simply reheated on the roll mill. Once the material is fed to the mill, the first pair of

rolls control the feeding rate, while subsequent rolls in the calender calibrate the sheet thickness. Most calender systems have four rolls as does the one in Fig. 6.82, which is an inverted L- or F-type system. Other typical roll arrangements are shown in Fig. 6.83 and 6.84. After passing through the main calender, the sheet can be passed through a secondary calendering operation for embossing. The sheet is then passed through a series of chilling rolls where it is cooled from both sides in an alternating fashion. After cooling, the film or sheet is wound.

One of the major concerns in a calendering system is generating a film or sheet with a uniform thickness distribution with tolerances as low as ±0.005 mm. To achieve this, the dimensions of the rolls must be precise. It is also necessary to compensate for roll bowing resulting from high pressures in the nip region. Roll bowing is a structural problem that can be mitigated by placing the rolls in a slightly crossed pattern, rather than completely parallel, or by applying moments to the roll ends to counteract the separating forces in the nip region.

Calendering can be modeled by assuming steady state, laminar flow and isothermal conditions.

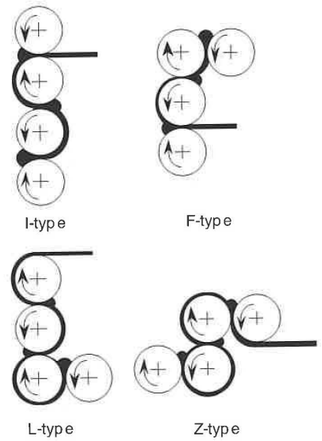

Figure 6.83 Calender arrangements.

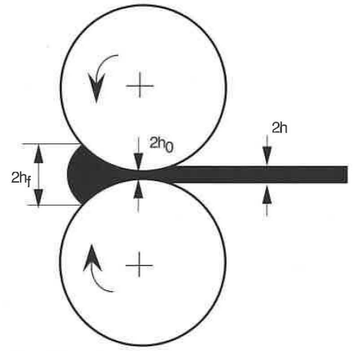

Figure 6.84 Schematic of the calendering process.

6.6 Coating

In coating a liquid film is continuously deposited on a moving, flexible or rigid substrate. Coating is done on metal, paper, photographic films, audio and video tapes, and adhesive tapes. Typical coating processes include *wire coating*, *dip coating*, *knife coating*, *roll coating*, *slide coating*, and *curtain coating*.

In wire coating, a wire is continuously coated with a polymer melt by pulling the wire through an extrusion die. The polymer resin is deposited onto the wire using the drag flow generated by the moving wire and sometimes a pressure flow generated by the back pressure of the extruder. The process is schematically depicted in Fig. 6.85[13]. The second normal stress differences, generated by the high shear deformation in the die, help keep the wire centered in the annulus [40].

Dip coating is the simplest and oldest coating operation. Here, a substrate is continuously dipped into a fluid and withdrawn with one or both sides coated with the fluid. Dip coating can also be used to coat individual objects that are dipped and withdrawn from the fluid. The fluid viscosity and density and the speed and angle of the surface determine the coating thickness.

13 Other wire coating processes extrude a tubular sleeve which adheres to the wire via stretching and vacuum. This is called tube coating.

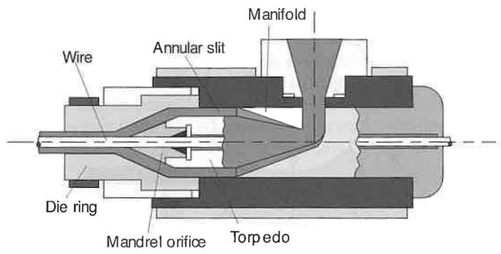

Figure 6.85 Wire coating process.

Knife coating, depicted in Fig. 6.86, consists of metering the coating material onto the substrate from a pool of material, using a fixed rigid or flexible knife. The knife can be normal to the substrate or angled and the bottom edge can be flat or tapered. The thickness of the coating is nearly half the gap between the knife edge and the moving substrate or web. A major advantage of a knife edge coating system is its simplicity and relatively low maintenance.

Roll coating consists of passing a substrate and the coating simultaneously through the nip region between two rollers. The physics governing this process is similar to calendering, except that the fluid adheres to both the substrate and the opposing roll. The coating material is a low viscosity fluid, such as a polymer solution or paint and is picked up from a bath by the lower roll and applied to one side of the substrate. The thickness of the coating can be as low as a few μm and is controlled by the viscosity of the coating liquid and the nip dimension. This process can be configured as either forward roll coating for co-rotating rolls or reverse roll coating for counter-rotating rolls (Fig. 6.87). The reverse roll coating process delivers the most accurate coating thicknesses.

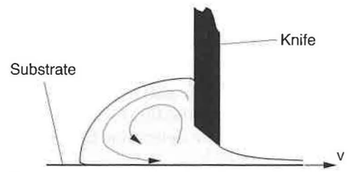

Figure 6.86 Schematic of a knife coating process.

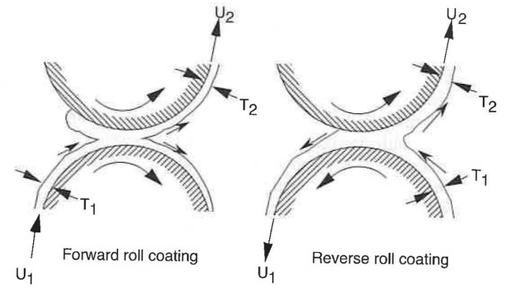

Figure 6.87 Schematic of forward and reverse roll coating processes.

Slide coating and curtain coating, schematically depicted in Fig. 6.88, are commonly used to apply multi-layered coatings. However, curtain coating has also been widely used to apply single layers of coatings to cardboard sheet. In both methods, the coating fluid is pre-metered.

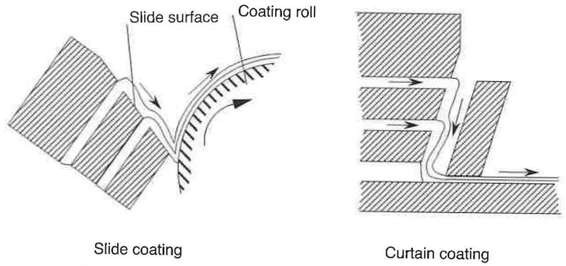

Figure 6.88 Slide and curtain coating.

6.7 Compression Molding

Compression molding is widely used in the automotive industry to produce parts that are large, thin, lightweight, strong, and stiff. It is also used in the household goods and electrical industries. Compression molded parts are formed by squeezing a charge, often glass fiber reinforced, inside a mold cavity, as depicted in Fig. 6.89. The matrix can be either a thermoset or thermoplastic. The oldest and still widest used material for compression molded products is phenolic. The thermoset materials used to manufacture fiber reinforced compression molded articles is unsaturated polyester sheet or bulk, reinforced with glass fibers, known as sheet molding compound (SMC) or bulk molding compound (BMC). In SMC, the 25 mm long reinforcing fibers are randomly oriented in the plane of the sheet and make up for 20-30% of the molding compound's volume fraction. A schematic diagram of an SMC production line is depicted in Fig. 8.90 [41]. When producing SMC, the chopped glass fibers are sandwiched between two carrier films previously coated with unsaturated polyester-filler matrix. A fiber reinforced thermoplastic charge is often called a glass mat reinforced thermoplastic (GMT) charge. The most common GMT matrix is polypropylene. More recently, long fiber reinforced themoplastics (LFT) have become common. Here, one squeezes sausage shaped charges deposited on the mold by an extruder.

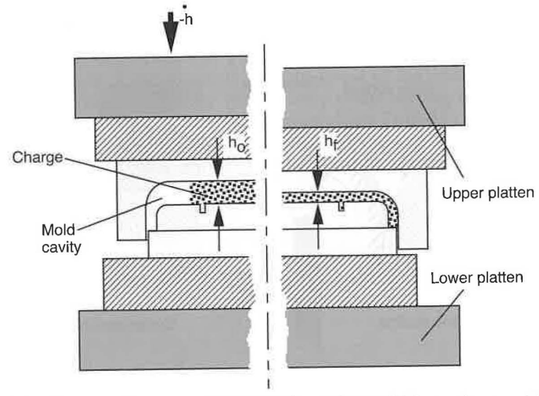

Figure 6.89 Compression molding process (h_0 = charge thickness, h_f = part thickness, and h= closing speed).

During processing of thermoset charges, the SMC blank is cut from a preformed roll and is placed between heated cavity surfaces. Generally, the mold is charged with 1 to 4 layers of SMC, each layer about 3 mm thick, which initially cover about half the mold cavity's surface. During molding, the initially randomly oriented glass fibers orient, leading to anisotropic properties in the finished product. When processing GMT charges, the preforms are cut and heated between radiative heaters. Once heated, they are placed inside a cooled mold that rapidly closes and squeezes the charges before they cool and solidify.

One of the main advantages of the compression molding process is the low fiber attrition during processing. Here, relatively long fibers can flow in the melt without the fiber damage common during plastication and cavity filling in injection molding.

An alternate process is injection-compression molding. Here, a charge is injected through a large gate followed by a compression cycle. The material used in the injection compression molding process is called bulk molding compound (BMC), which is reinforced with shorter fibers, generally 1 cm long, with an unsaturated polyester matrix. The main benefit of injection compression molding over compression molding is automation. The combination of injection and compression molding leads to lower degrees of fiber orientation and fiber attrition compared to injection molding.

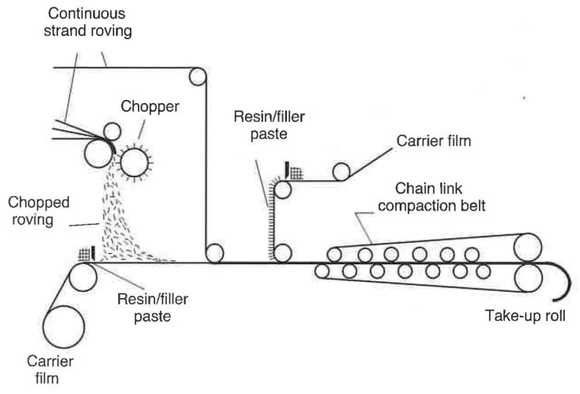

Figure 6.90 SMC production line.

6.8 Foaming

In foam or a foamed polymer, a cellular or porous structure has been generated through the addition and reaction of *physical* or *chemical blowing agents*. The basic steps of foaming are cell nucleation, expansion or cell growth, and cell stabilization. Nucleation occurs when, at a given temperature and pressure, the solubility of a gas is reduced, leading to saturation, expelling the excess gas to form a bubble. Nucleating agents, such as powdered metal oxides, are used for initial bubble formation. The bubbles reach an equilibrium shape when their inside pressure balances their surface tension and surrounding pressures. The cells formed can be completely enclosed (closed cell) or can be interconnected (open cell).

A physical foaming process is one where a gas such as nitrogen or carbon dioxide is introduced into the polymer melt. Physical foaming also occurs after heating a melt that contains a low boiling point fluid, causing it to vaporize. For example, the heat-induced volatilization of low-boiling-point liquids, such as pentane and heptane, is used to produce polystyrene foams. Also, foaming occurs during volatilization from the exothermic reaction of gases produced during polymerization such as the production of carbon dioxide during the reaction of isocyanate with water. Physical blowing agents are added to the plasticating zone of the extruder or molding machine. The most widely used physical blowing agent is nitrogen. Liquid blowing agents are often added to the polymer in the plasticating unit or the die.

Chemical blowing agents are usually powders introduced in the hopper of the molding machine or extruder. Chemical foaming occurs when the blowing agent thermally decomposes, releasing large amounts of gas. The most widely used chemical blowing agent for polyolefin is azodicarbonamide.

In mechanical foaming, a gas dissolved in a polymer expands upon reduction of the processing pressure.

The foamed structures commonly generated are either homogeneous foams or integral foams. Figure 6.91 [42] presents the various types of foams and their corresponding characteristic density distributions. In integral foam, the unfoamed skin surrounds the foamed inner core. This type of foam can be achieved during injection molding and extrusion and it replaces the sandwiched structure also shown in Fig. 6.91.

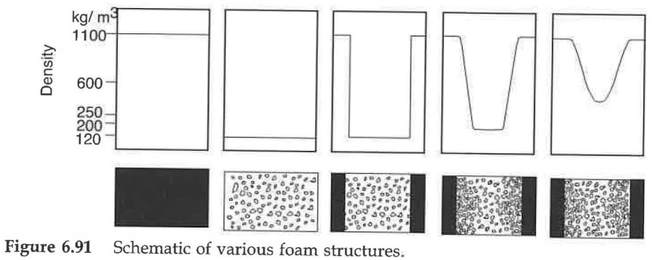

Figure 6.91 Schematic of various foam structures.

Today, foams are of great commercial importance and are primarily used in packaging and as heat and noise insulating materials. Examples of foamed materials are polyurethane foams, expanded polystyrene (EPS) and expanded polypropylene particle foam (EPP).

Polyurethane foam is perhaps the most common foaming material and is a typical example of a chemical foaming technique. Here, two low viscosity components, a polyol and an isocyanate, are mixed with a blowing agent such as pentane. When manufacturing semi-finished products the mixture is deposited on a moving conveyor belt where it is allowed to rise, like a loaf of bread contained whithin shaped paper guides. The result is a continuous polyurethane block that can be used, among others, in the upholstery and matress industries.

The basic material to produce expanded polystyrene products are small pearls produced by suspension styrene polymerization with 6-7% of pentane as a blowing agent. To process the pearls they are placed in pre-expanding machines heated with steam until their temperature reaches 80 to 100 °C. To enhance their expansion, the pearls are allowed to cool in a vacuum and allowed to age and dry in ventilated storage silos before the shaping operation. Polystyrene foam is is used extensively in packaging, but its uses also extend to the construction industry as a thermal insulating material, as well as for shock absorption in children's safety seats and bicycle helmets.

Expanded polypropylene particle foam is similar in to EPS but is characterized by its excellent impact absorption and chemical resistance. Its applications are primarely in the automotive industry as bumper cores, sun visors and knee cushions, to name a few.

6.9 Rotational Molding

Rotational molding is used to make hollow objects. In rotational molding, a carefully measured amount of powdered polymer, typically polyethylene, is placed in a mold. The mold is then closed and placed in an oven where the mold turns about two axes as the polymer melts, as depicted in Fig. 6.92. During heating and melting, which occur at oven temperatures between 250 and 450 °C, the polymer is deposited evenly on the mold's surface. To ensure uniform thickness, the axes of rotation should not coincide with the centroid of the molded product. The mold is then cooled and the solid part is removed from the mold cavity. The parts can be as thick as 1 cm, and still be manufactured with relatively low residual stresses. The reduced residual stress and the controlled dimensional stability of the rotational molded product depend in great part on the cooling rate after the mold is removed from the oven. A mold that is cooled too fast yields warped parts. Usually, a mold is first cooled with air to start the cooling slowly, followed by a water spray for faster cooling.

The main advantages of rotational molding over blow molding are the uniform part thickness and the low cost involved in manufacturing the mold. In addition, large parts such as play structures or kayaks can be manufactured more economically than with injection molding or blow molding. The main disadvantage of the process is the long cycle time for heating and cooling of the mold and polymer.

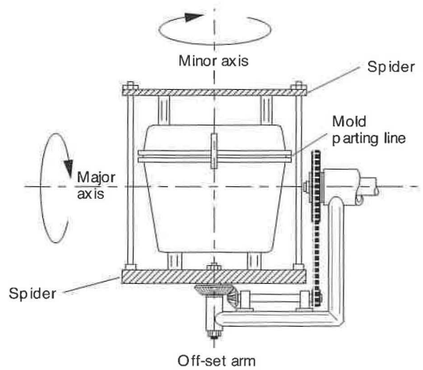

Figure 6.92 Schematic of the rotational molding process.

Figure 6.93 presents the air temperature inside the mold in a typical rotational molding cycle for polyethylene powders [43]. The process can be divided into six distinct phases:

1. Induction or initial air temperature rise
2. Melting and sintering
3. Bubble removal and densification
4. Pre-cooling
5. Crystallization of the polymer melt
6. Final cooling

The induction time can be significantly reduced by pre-heating the powder, and the bubble removal and cooling stage can be shortened by pressurizing the material inside the mold. The melting and sintering of the powder during rotational molding depends on the rheology and geometry of the particles. This phenomenon was studied in depth by Bellehumeur and Vlachopoulos [44].

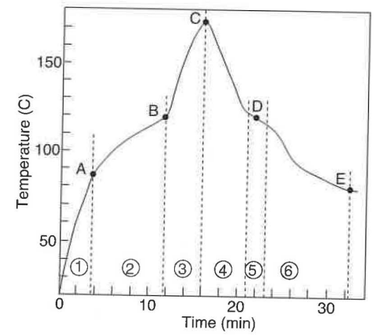

Figure 6.93 Typical air temperature in the mold while rotomolding polyethylene parts.

Examples

6.1 You are to use a 45 mm diameter single screw extruder to create a polymer polycarbonate/polypropylene polymer blend. The maximum screw rotation is 160 rpm and the screw channel depth is 4mm. Assuming a barrel temperature of 300 °C, a surface tension, between the two polymers of $8x10^{-3}$ N/m, and using the viscosity curves given in in the appedix of this book, determine:

- If one can disperse 20% PC into 80% PP
- If one can disperse 20% PP into 80% PC
- The minimum size of the dispersed phase

We start this problem by first calculating the average speed in the extruder using

$$v_0 = \pi Dn = \pi(45)(160)(1/60) = 377\,\text{mm/s}$$

which results in an average rate of deformation of

$$\dot{\gamma} = \frac{v_0}{h} = \frac{377\,\text{mm/s}}{4\,\text{mm}} = 94\,\text{s}^{-1}$$

From the viscosity curves we get $\eta_{PC} \approx 600\,\text{Pa}-\text{s}$ and $\eta_{PP} \approx 150\,\text{Pa}-\text{s}$. Using Fig. 6.32 we can deduce that one cannot disperse polycarbonte into polypropylene using a single screw extruder that only induces shear deformation, since $\eta_{PC}/\eta_{PP} > 4$. On the other hand, one can disperse polypropylene into polycarbonate using the same single screw extruder.

Using Fig.6.32 we can see that dispersive mixing for a $\eta_{PC}/\eta_{PP} > 0.25$ will occur at $Ca_{crit} \approx 0.7$. Hence, neglecting the effects of coalescence we can calculate the minimun size of the dispersed phase using

$$Ca_{crit} = 0.7 = \frac{\tau R}{\sigma_s} = \frac{600(94)R}{8x10^{-3}} \rightarrow D = 2R = 0.2\mu m$$

To achieve this dispersion we must maintain the stresses for an extended period.

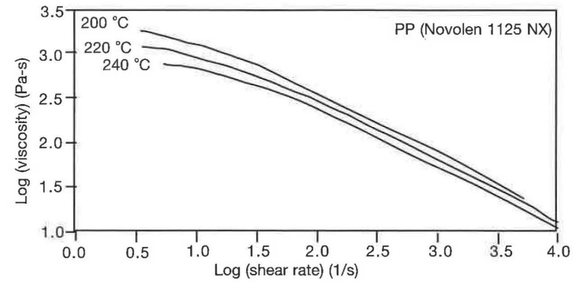

Figure 6.94 Viscosity curves for a polypropylene.

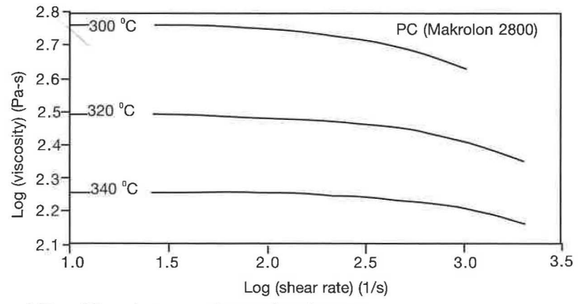

Figure 6.95 Viscosity curves for a polycarbonate.

6.2 You are to determine the maximum clamping force and injection pressure required to mold an ABS suitcase with a filling time, t_{fill}, of 2.5 seconds. Use the dimensions shown in Fig. 6.96, an injection temperature, T_i, of 227 °C (500 K), and a mold temperature, T_m, of 27 °C (300 K). The properties necessary for the calculations are also given below.

Table 6.8 Properties for ABS

$n = 0.29$	$\rho = 1020\,\text{kg/m}^3$
$m_0 = 29x10^6\,\text{Pa}-\text{s}^n$	$C_p = 2343\,\text{J/Kg/K}$
$a = 0.01369\,\text{/K}$	$k = 0.184\,\text{W/m/K}$

To aid the polymer processing engineer in finding required injection pressures and corresponding mold clamping forces, Stevenson [4] generated a set of dimensionless groups and corresponding graphs for non-isothermal mold filling of non-Newtonian polymer melts. We start this problem by first laying the suitcase flat and determining the required geometric factors (Fig. 6.97). From the suitcase geometry, the longest flow path, , is 0.6 m and the radius of the projected area, R_p, is 0.32 m.

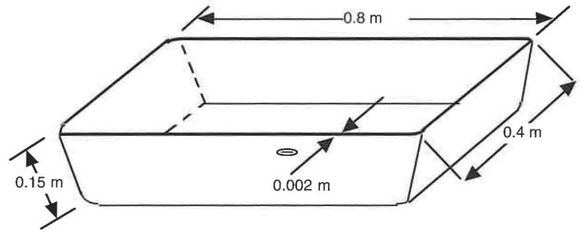

Figure 6.96 Suitcase geometry.

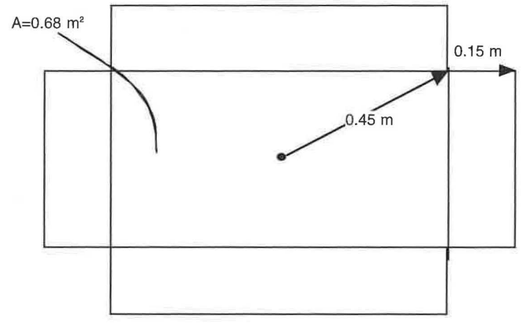

Figure 6.97 Layed-flat suitcase.

Using the notation in Fig. 6.25 and a viscosity defined by $\eta = m_0 e^{-a(T-T_{ref})}|\dot{\gamma}|^{n-1}$, four dimensionless groups are defined.

- The dimensionless temperature β determines the intensity of the coupling between the energy equation and the momentum balance. It is defined by

$$\beta = a(T_i - T_m) \tag{6.30}$$

where T_i and T_m are the injection and mold temperatures respectively.

- The dimensionless time is the ratio of the filling time, t_{fill}, and the time for thermal equilibrium via conduction, defined by

$$\tau = \frac{t_{fill} K}{h^2 \rho C_p} \tag{6.31}$$

- The Brinkman number Br is the ratio of the energy generated by viscous dissipation and the energy transported by conduction. For a non-isothermal, non-Newtonian model it is

$$Br = \frac{m_0 e^{-aT_i} h^2}{k(T_i - T_m)} \left(\frac{R}{t_{fill} h}\right)^{n+1} \tag{6.32}$$

- The power-law index n of the Ostwald and deWaale model reflects the shear thinnng behavior of the polymer melt. Once the dimensionless parameter are calculated, the dimensionless injection pressures $(\Delta p/\Delta p_I)$ and dimensionless clamping forces (F/F_I) are read from Figs. 6.98 to 6.101. The isothermal pressure and force are computed using

$$\Delta p_I = \frac{m_0 e^{-aT_i}}{1-n} \left[\frac{1+2n}{2n} \frac{R}{t_{fill} h}\right]^n \left(\frac{R}{h}\right) \tag{6.33}$$

and

$$F_I = \pi R^2 \left(\frac{1-n}{3-n}\right) \Delta p_I \tag{6.34}$$

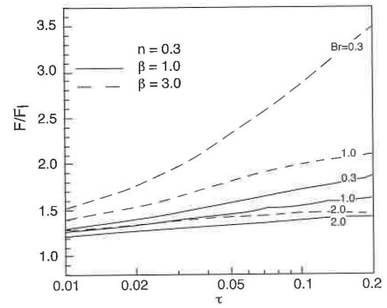

Figure 6.98 Dimensionless clamping force versus dimensionless groups.

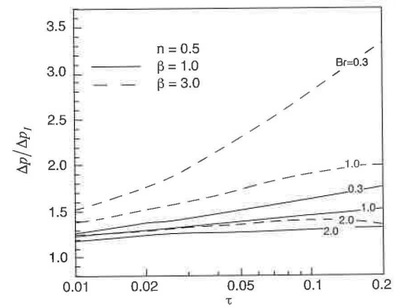

Figure 6.99 Dimensionless clamping force versus dimensionless groups.

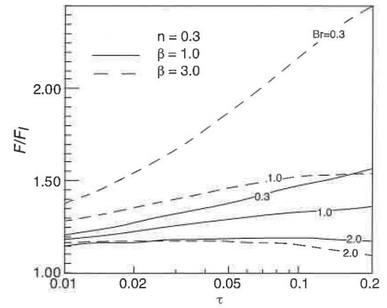

Figure 6.100 Dimensionless injection pressure versus dimensionless groups.

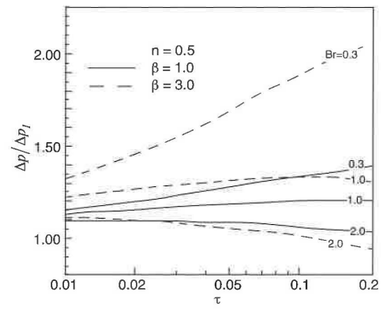

Figure 6.101 Dimensionless injection pressure versus dimensionless groups.

Using the data given for ABS and the dimensions for the laid-flat suitcase we can compute the dimensionless groups as

$$\beta = 0.01369(500 - 300) = 2.74$$

$$\tau = \frac{2.5(0.184)}{(0.001)^2(1020)(2343)} = 0.192$$

$$Br = \frac{(29x10^6)e^{-0.01369(500)}(0.001)^2}{0.184(500-300)}\left(\frac{0.6}{2.5(0.001)}\right)^{0.29+1} = 0.987$$

The isothermal injection pressure and clampng force are computed using eqs. 6.30 to 6.34.

$$\Delta p_I = \frac{29x10^6 e^{-0.01369(500)}}{1-0.29}\left(\frac{1+2(0.29)}{2(0.29)}\frac{0.6}{2.5(0.001)}\right)^{0.29}\left(\frac{0.6}{0.001}\right) = 171\text{MPa}$$

$$F_I = \pi(0.6)^2\left(\frac{1-0.29}{3-0.29}\right)(17.1x10^7) = 50.7x10^6\text{N}$$

We now look up $\Delta p/\Delta p_I$ and F/F_I in Figs. 6.98 to 6.101. Since little change occurs between n = 0.3 and n = 0.5, we choose n = 0.3. However, for other values of n we can interpolate or extrapolate. For $\beta = 2.74$, we interpolate between 1 and 3 as

$$\beta = 1 \rightarrow \Delta p/\Delta p_I = 1.36 \text{ and } F/F_I = 1.65$$

$$\beta = 3 \rightarrow \Delta p/\Delta p_I = 1.55 \text{ and } F/F_I = 2.1$$

$$\beta = 2.74 \rightarrow \Delta p/\Delta p_I = 1.53 \text{ and } F/F_I = 2.04$$

$$\Delta p = \left(\Delta p/\Delta p_I\right)\Delta p_I = 262\text{MPa} = 2{,}620\text{bar}$$

$$F = \left(F/F_I\right)F_I = 10.3x10^7\text{N} = 10{,}300\,\text{metric tons}$$

Since the part are exceeds the projected area, Fig. 6.102 can be used to correct the computed clamping force. The clamping force can be corrected forn an R_p= 0.32 m using Fig. 6.102 and $R_p/R = 0.53$.

$$F_{projected} = (0.52)10{,}300 = 5{,}356\text{metric tons}$$

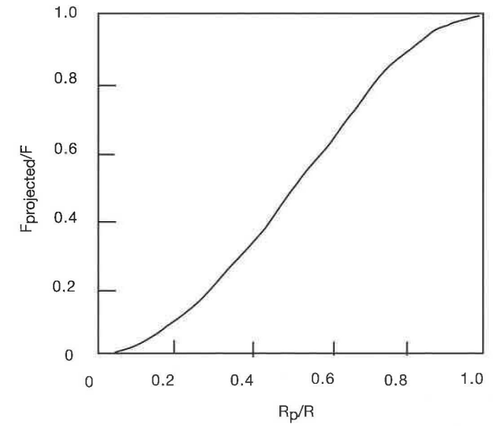

Figure 6.102 Clamping force correction for the projected area.

For our suitcase cover, where the total volume is 1,360 cc and total part area is 0.68 m^2, the above numbers are too high. A usefull rulo-of-thumb is a maximun allowable clamping force of 2 tons/in^2. Here, we have gratly exceeded that number. Normally, around 3,000 metric tons/m^2 are allowed in commercial injection molding machines. For example, a typical injection molding machine[14] with a shot size of 2,000 cc has a maximun clamping force of 630 metric tons with a maximun injection pressure of 1,400 bar. A machine with much larger clamping forces and injection pressures is suitable for much larger parts. For example, a mchaine with a shot size of 19,000 cc allows a maximum clamping force of 6,000 metric tons with a maximum injection pressure of 1,700 bar. For this example we must reduce the pressure and

14 MINIFLOW, Injection Molding Simulation, The Madison Groups PPRC, Madison, WI.

clamping force requirements. This can be acomplished by increasing the injection and mold temperatures or by reducing the filling time. Recommended injection temperatures for ABS are between 210 and 240 °C and recommended mold temperatures are between 40 and 90 °C.[15] As can be seen, there is room for adjustment in the processing condition, so one must repeat the above procedure using new conditions.

6.3 Let us consider the multi-cavity injection molding process shown in Fig. 6.103. To achieve equal part quality, the filling time for all cavities must be balanced. For the case in question, we need to balance the cavities by solving for the runner radius. For a balanced runner system the flow rates into all cavities must match. For a given flow rate Q, length L, and radius R_1, we can also solve for the pressure at the runner system junctures. Assuming an isothermal flow of a non-Newtonian shear thinning polymer with viscosity η, we can compute the radius for a part molded of polystyrene with a consistency index of $2.8x10^4$ Pa – s^n and a power law index (n) of 0.28.

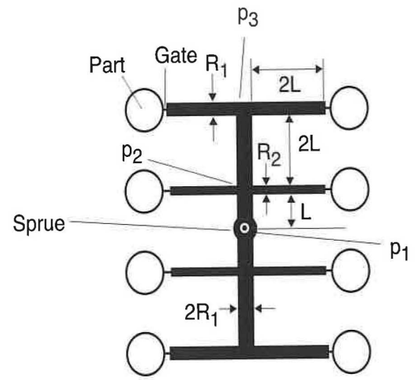

Figure 6.103 Runner system lay out.

The flow through each runner section is governed by equation 5.46, and the various sections can be represented using:

15 A good reference for such values is the CAMPUS® material data bank. Books such as H. Domininghaus, *Plastics for Engineers*, Hanser Publishers (1992), Munich are also recommended.

Section 1: $$4Q = \left(\frac{\pi(2R_1)^3}{s+3}\right)\left(\frac{2R_1(P_1-P_2)}{2mL}\right)^s$$

Section 2: $$2Q = \left(\frac{\pi(2R_1)^3}{s+3}\right)\left(\frac{2R_1(P_2-P_3)}{2m(2L)}\right)^s$$

Section 3: $$Q = \left(\frac{\pi R_2^3}{s+3}\right)\left(\frac{R_2(P_2-0)}{2m(2L)}\right)^s$$

Section 4: $$Q = \left(\frac{\pi R_1^3}{s+3}\right)\left(\frac{R_1(P_3-0)}{2m(2L)}\right)^s$$

Using values of $L = 10$cm, $R_1 = 4$mm mm, and $Q = 20cm^3/s$, the unknown parameters, P_1, P_2, P_3, and R_2 can be obtained using the preciding equations. The equation are non-linear and must be solved in an iterative manner. For the given values, a radius, R_2, of 3.4 mm would result in a balanced runner system, with pressures P_1 = 265.7 bar, P_2 = 230.3 bar, and P_3 = 171.9 bar. For comparison, if one had assumed a Newtonian model with the same consistency index and a power law index of 1.0 a radius, R_2, of 3.9 mm would have resulted, with much higher required pressures of P_1 = 13,926 bar, P_2 = 12,533 bar, and P_3 = 11,140 bar. The difference is due to shear thinning.

Problems

6.1 You are to extrude a 100 mm wide high density polyethylene sheet using a 40 mm diameter single screw extruder with distributive as well as dispersive mixing heads. The screw characteristic curve is shown in Fig. 6.104[16].

The die can be approximated with a 100 mm wide and 100 mm long slit. On the graph below draw the die characteristic curves for dies with 1mm and 1.5mm thick slits. Will it be feasible to extrude a sheet through a 1.5mm thick slit? If yes, what screw speed would you choose? What about a 1 mm thick slit.

16 Courtesy of ICIPC, Medellín, Colombia.

Why do your die characteristic curves cross over the ones shown in the graph? Note that the data in the graph was measured experimentally with a variable restriction (valve) die.

Typical power law constants for HDPE at 180 °C are m=20,000 Pa-s^n and n=0.41. Use a specific gravity for HDPE of 0.95.

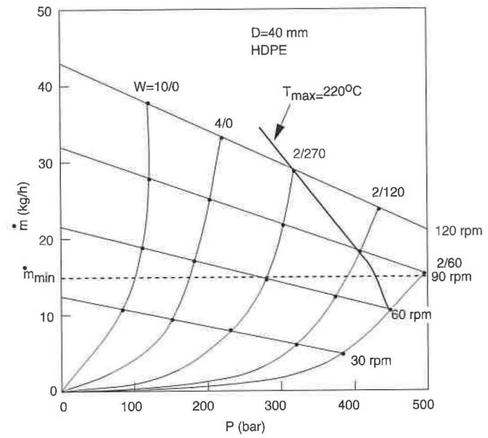

Figure 6.104 Process characteristic curves for a 45 mm diameter conventional extruder.

6.2 Estimate the striation thickness of a 3mm diameter pigmented polystyrene pellet in a polystyrene matrix after traveling through a 20 turn, 45 mm diameter, 5 mm constant channel depth, single screw extruder. Assume open discharge conditions. Use 100 rpm rotational speed.

6.3 Someone in your company proposes to use an existing square pitch 150 mm diameter plasticating single screw extruder as a mixing device for a 40/60 PS/PP polymer blend. The metering section is 5 turns long and has a channel depth of 10 mm. Will dispersion of the polystyrene occur for a screw rotation of 60 rpm? Assume open discharge and a temperature of 220 °C. Use viscosity data given in example 6.1 and Fig. 6.106.

6.4 Someone in your company proposes to use an existing square pitch 150 mm diameter plasticating single screw extruder as a mixing device for a 40/60 PP/PS polymer blend. The metering section is 5 turns long and has a channel depth of 10 mm. Will dispersion of the polypropylene occur for a screw rotation of 60 rpm? Will there be enough time for dispersion? Assume open discharge and a temperature of 220 °C. Use viscosity data given in problems 6.3 and below.

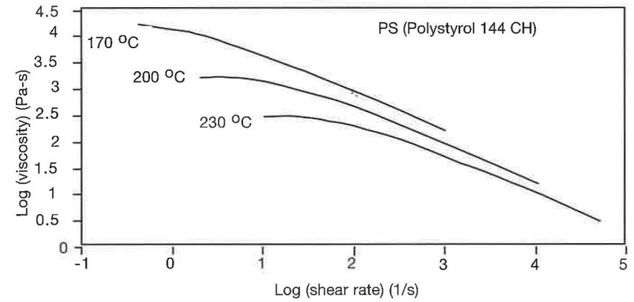

Figure 6.105 Viscosity curves for a polystyrene.

6.5 A thin polyamide 66 component is injection molded under the following conditions:

- The melt is injected at 275 °C to a maximum pack/hold pressure of 800 bar.
- The 800 bar pack/hold pressure is maintained until the gate freezes off, at which point the part is at an average temperature of 175 °C.
- The pressure drops to 1 bar as the part cools inside the cavity.
- The part is removed from the mold and cooled to 25 °C.
- Draw the whole process on the PvT diagram.
- Estimate the final part thickness if the mold thickness is 1 mm. For thin injection molded parts, most of the shrinkage leads to part thickness reduction.

6.6 Does the screw and die characteristic curves, correspond to a conventional or a grooved single screw extruder?

A die can be approximated with a 1 mm diameter and 30 mm long

capillary. On the graph below draw the die characteristic curve for the given die?

Typical power law constants for HDPE at 180 °C are m=20,000 Pa-s^n and n=0.41. Use a specific gravity for HDPE of 0.95.

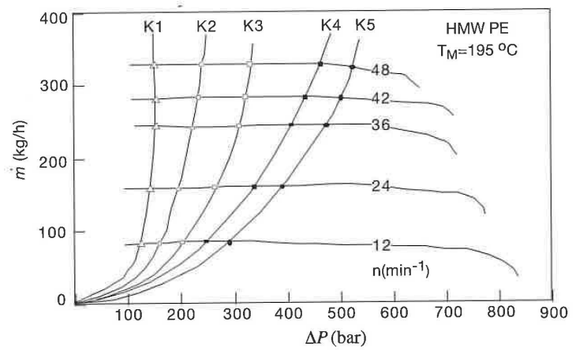

Figure 6.106 Process characteristic curves for a 45 mm diameter extruder.

6.7 An internal batch mixer maintains shear rates, $\dot{\gamma}$, of 100 s^{-1} for extended periods. In the mixer you want to disperse LDPE in a PS matrix at 170 °C. What is the size of the dispersed phase? Will the PS still be transparent? Use viscosity data given in Problem 6.4 and below.

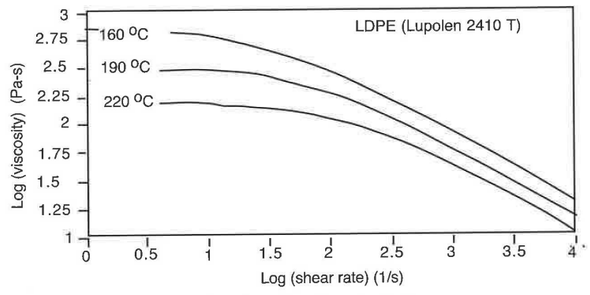

Figure 6.107 Viscosity curves for a low density polyethylene.

6.8 Design a balanced runner system for the mold in Example 6.3 if you are to injection mold a polystyrene product. Assume a power-law model with a consistency index, m, of 2.8x10^4 Pa-s^n, and a power-law index, n, of 0.28.

6.9 Estimate the cooling time for the ABS suitcase presented in Example 6.2 if demolding occurs when the average part temperature is below 60 °C.

6.10 What are the required clamping force and injection pressure if the filling time in Example 6.2 is increased from 2.5 s to 3 s?

6.11 What are the required clamping force and injection pressure if the mold temperature in Example 6.2 is increased from 27 °C to 90 °C ?

6.12 What are the required clamping force and injection pressure if the injection temperature in Example 6.2 is increased from 227 to 240 °C?

6.13 Measure and plot the wall thickness distribution on a PE-HD one gallon milk container.

6.14 Measure and plot the wall thickness distribution on a small thermoformed individual coffee cream container.

References

1. Tadmor, Z., and Gogos, C.G., Principles of Polymer Processing, John Wiley & Sons, New York, (1979).
2. Rauwendaal, C., *Mixing in Polymer Processing*, Marcel Dekker, Inc., New York, (1991).
3. Osswald, T.A., Turng, L.S., and Gramann, P.J., Injection Molding Handbook, Hanser Publishers, Munich, (2001).
4. Menges, G., and Predöhl, W., *Plastverarbeiter, 20*, 79, (1969).
5. Menges, G., and Predöhl, W., *Plastverarbeiter, 20*, 188, (1969).
6. Scott, C.E., and Macosko, C.W., *Polymer Bulletin, 26*, 341, (1991).
7. Gramann, P.J., Stradins, L., and Osswald, T.A., *Intern. Polymer Processing*, 8, 287, (1993).
8. Osswald, T.A., *Polymer Processing Fundamentals*, Hanser Publishers, Munich, (1998).
9. Erwin, L., *Polym. Eng. & Sci., 18*, 572, (1978).
10. Erwin, L., *Polym. Eng. & Sci., 18*, 738, (1978).
11. Ng, K.Y., Master of Science Thesis, University of Wisconsin-Madison, (1979).
12. Tadmor, Z., *Ind. Eng. Fundam., 15*, 346, (1976).

13. Cheng, J., and Manas-Zloczower, I., *Internat. Polym. Proc.*, 5, 178, (1990).
14. Grace, H.P., *Chem. Eng. Commun., 14*, 225, (1982).
15. Cox, R.G., *J. Fluid Mech.*, 37, 3, 601–623, (1969).
16. Bentley, B.J. and Leal, L.G., *J. Fluid Mech.*, 167, 241–283, (1986).
17. Stone, H.A. and Leal, L.G., *J. Fluid Mech.*, 198, 399–427, (1989).
18. Biswas, A., and Osswald, T.A., unpublished research, (1994).
19. Gramann, P.J., M.S. Thesis, University of Wisconsin-Madison, (1991).
20. Manas-Zloczower, I., Nir, A., and Tadmor, Z., *Rubber Chemistry and Technology*, 55, 1250, (1983).
21. Boonstra, B.B., and Medalia, A.I., *Rubber Age*, March and April, (1963).
22. Rauwendaal, C., *Polymer Extrusion*, Hanser Publishers, Munich, (1990).
23. Menges, G., and Harms, E., *Kautschuk und Gummi, Kunststoffe, 25*, 469, (1972).
24. Rauwendaal, C., *SPE ANTEC Tech. Pap., 39*, 2232, (1993).
25. Rauwendaal, C., *Mixing in Reciprocating Extruders*, A chapter in *Mixing and Compounding of Polymers*, Eds. I. Manas-Zloczower and Z. Tadmor, Hanser Publishers, Munich, (1994).
26. Elemans, P.H.M., Modeling of the cokneater, A chapter in *Mixing and Compounding of Polymers*, Eds. I. Manas-Zloczower and Z. Tadmor, Hanser Publishers, Munich, (1994).
27. Lim, S. and White, J.L., *Intern. Polymer Processing, 8*, 119, (1993).
28. Lim, S. and White, J.L., *Intern. Polymer Processing, 9*, 33, (1994).
29. Bird, R.B., Steward, W.E., and Lightfoot, E.N., *Transport Phenomena*, John Wiley & Sons, New York, (1960).
30. Erwin, L., *Polym. Eng. & Sci., 18*, 1044, (1978).
31. Suetsugu, *Intern. Polymer Processing, 5*, 184, (1990).
32. Greener, J., *Polym. Eng. Sci., 26*, 886 (1986).
33. Michaeli, W., and Lauterbach, M., *Kunststoffe , 79*, 852 (1989).
34. Stevenson, J.F., *Polym. Eng. Sci., 18*, 577 (1978).
35. Osswald, T.A., and Menges, G., *Materials Science of Polymers for Engineers*, Hanser Publishers, Munich (1996).
36. Anturkar, N.R., and Co, A., *J. Non-Newtonian Fluid Mech., 28*, 287 (1988).
37. Menges, G., *Einführung in die Kunststoffverarbeitung*, Hanser Publishers, Munich (1986).
38. Rosato, D.V., *Blow Molding Handbook*, Hanser Publishers, Munich (1989).
39. Modern Plastics Encyclopedia, 53, McGraw-Hill , New York (1976).
40. Tadmor, Z., and Bird, R.B., *Polym.Eng.Sci, 14*, 124 (1973).
41. Denton, D.L., *The Mechanical Properties of an SMC-R50 Composite*, Owens-Corning Fiberglas Corporation (1979).
42. Shutov, F.A., *Integral/Structural Polymer Foams*, Springer-Verlag, Berlin (1986).
43. Crawford, R.J., *Rotational Molding of Plastics*, Research Studies Press, Somerset (1992).
44. Bellehumeur, C.T., and Vlachopoulos, J., *SPE 56th Antec*, (1998).
45. Mascia, L., *The Role of Additives in Plastics*, John Wiley & Sons, New York, (1974).
46. Hildebrand, J. and Scott, R.L., *The Solubility of Non-Electrolytes*, 3rd Ed., Reinhold. Publishing Co., New York, (1949).
47. Rosen, S.L., *Fundamental Principles of Polymeric Materials*, 2nd. Ed., John Wiley & Sons, Inc., New York, (1993).

48. Janssen, J.M.H., Ph.D. Thesis, Eindhoven University of Technology, The Netherlands, (1993).
49. van Krevelen, D. W., and Hoftyzer, P.J., *Properties of Polymers*, 2nd ed., Elsevier, Amsterdam, (1976).